nature immunology

ZAPS is a potent stimulator of signaling mediated by the RNA helicase RIG-I during antiviral responses

Sumio Hayakawa[1,8], Souichi Shiratori[1,2,8], Hiroaki Yamato[1,3,8], Takeshi Kameyama[1], Chihiro Kitatsuji[1], Fumi Kashigi[1,7], Showhey Goto[1,7], Shoichiro Kameoka[1,7], Daisuke Fujikura[4], Taisho Yamada[1], Tatsuaki Mizutani[5], Mika Kazumata[1], Maiko Sato[1], Junji Tanaka[2], Masahiro Asaka[3], Yusuke Ohba[5], Tadaaki Miyazaki[4], Masahiro Imamura[2] & Akinori Takaoka[1,6]

The poly(ADP-ribose) polymerases (PARPs) participate in many biological and pathological processes. Here we report that the PARP-13 shorter isoform (ZAPS), rather than the full-length protein (ZAP), was selectively induced by 5′-triphosphate–modified RNA (3pRNA) and functioned as a potent stimulator of interferon responses in human cells mediated by the RNA helicase RIG-I. ZAPS associated with RIG-I to promote the oligomerization and ATPase activity of RIG-I, which led to robust activation of IRF3 and NF-κB transcription factors. Disruption of the gene encoding ZAPS resulted in impaired induction of interferon-α (IFN-α), IFN-β and other cytokines after viral infection. These results indicate that ZAPS is a key regulator of RIG-I signaling during the innate antiviral immune response, which suggests its possible use as a therapeutic target for viral control.

Pathogen invasion is sensed by pattern-recognition receptors (PRRs) of the innate immune system through the recognition of pathogen-associated molecular patterns. Some subsets of the PRRs trigger the activation of intracellular signaling pathways, which leads to the induction of antimicrobial genes. The repertoire of such signal-transducing–type PRRs includes membrane-bound Toll-like receptors (TLRs) and C-type lectin receptors, as well as cytosolic receptors such as RNA helicase RIG-I–like receptors and Nod-like receptors[1–3]. Nucleic acids derived from viruses are key signatures that trigger antiviral defense against viral infection. Among those nucleic acids, viral RNA can serve as a major pathogen-associated molecular pattern targeted by TLR3, TLR7and TLR8 on the endosomal membrane and by RIG-I-like receptors in the cytosolic space.

At least three DExD–H-box RNA helicases[4,5], RIG-I, Mda5 and LGP2, are included in the RIG-I-like receptor family. RIG-I is a key PRR for the detection of positive- and negative-stranded RNA viruses in the cytoplasm of cells[6,7] and has an important role in triggering responses to many viruses, such as those of the orthomyxovirus family (influenza A virus), paramyxovirus family (measles, mumps and Sendai virus), hepatitis C virus and Japanese encephalitis virus[8]. RNA containing 5′-triphosphate modification (3pRNA) is essential for RIG-I recognition and activation[9,10]. Ligand binding activates the ATPase activity of RIG-I to change its structural conformation[6], which in turn enables RIG-I to interact through its amino-terminal tandem caspase-recruitment domain (CARD) with the adaptor protein MAVS (mitochondrial antiviral signaling protein; also known as IPS-1, VISA or Cardif)[11–14]. MAVS then initiates activation of the interferon-regulatory factor 3 (IRF3), IRF7 and NF-κB transcription factors and the subsequent production of type I interferons and inflammatory cytokines, which are crucial for activating innate immune responses to viral infection[6,15]. Given the important role of the RIG-I pathway in the antiviral innate response, the mechanisms that regulate RIG-I activation represent a topic of intense research[16–18].

Poly(ADP-ribose) polymerases (PARPs), which are a superfamily with least 17 members, are known to regulate not only cell-survival and cell-death programs triggered by DNA damage but also other biological functions, as well as pathological processes, such as inflammatory and degenerative diseases, in a manner dependent or independent of their PARP activity[19–22]. Several PARP superfamily members have a direct regulatory effect on the replication of certain viruses[19,20,22,23]. For example, PARP-1 directly poly(ADP-ribosyl)ates the Epstein-Barr virus–encoded origin-binding protein EBNA1 and the Kaposi's sarcoma–associated herpesvirus–encoded latency-associated nuclear antigen LANA and disables their functions[23,24]. PARP-13 (also known as ZAP (zinc-finger CCCH-type antiviral protein 1)) interacts with viral RNA from certain subsets of viruses, such as Moloney murine leukemia virus and Sindbis virus, and recruits the RNA exosome and the DEAD-box RNA helicase p72 to efficiently degrade RNA[20,25,26].

[1]Division of Signaling in Cancer and Immunology, Institute for Genetic Medicine, Hokkaido University, Sapporo, Japan. [2]Department of Hematology and Oncology, Hokkaido University Graduate School of Medicine, Sapporo, Japan. [3]Department of Gastroenterology, Hokkaido University Graduate School of Medicine, Sapporo, Japan. [4]Department of Bioresources, Hokkaido University Research Center for Zoonosis Control, Sapporo, Japan. [5]Laboratory of Pathophysiology and Signal Transduction, Hokkaido University Graduate School of Medicine, Sapporo, Japan. [6]Research Center of Infection-Associated Cancer, Institute for Genetic Medicine, Hokkaido University, Sapporo, Japan. [7]Department of Chemistry, Graduate School of Science, Hokkaido University, Sapporo, Japan. [8]These authors contributed equally to this work. Correspondence should be addressed to A.T. (takaoka@igm.hokudai.ac.jp).

Received 4 August; accepted 28 October; published online 21 November 2010; corrected online 8 December 2010 (details online); doi:10.1038/ni.1963

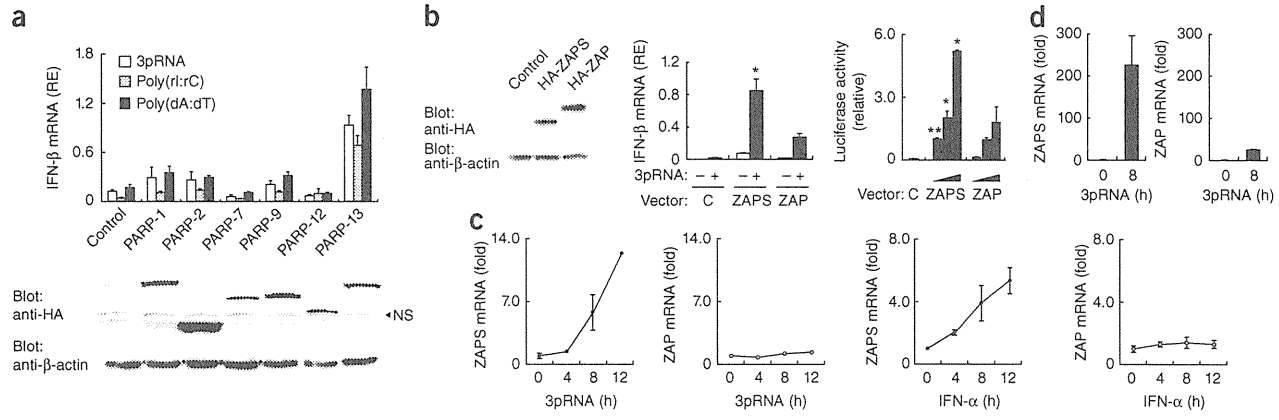

Figure 1 Involvement of PARP-superfamily members in interferon responses to cytosolic nucleic acids. (**a**) Quantitative RT-PCR analysis (top) of the induction of human IFN-β mRNA by stimulation with 3pRNA, poly(rI:rC) or poly(dA:dT) (1 μg/ml) in HEK293T cells transfected with control vector or expression vectors for various members of the mouse PARP family; results are presented in relative expression units (RE), relative to the expression of *ACTB* (encoding β-actin). Below, immunoblot analysis of PARP expression with antibody to hemagglutinin (anti-HA) or anti-β-actin (lanes correspond to bars above). NS, nonspecific band. (**b**) Quantitative RT-PCR analysis (middle) of IFN-β mRNA after 8 h of no stimulation (–) or stimulation with 3pRNA (+), and luciferase activity (right) of a p-125Luc firefly luciferase reporter plasmid at 48 h after transfection of HEK293T cells with increasing doses (wedges) of control vector (C) or expression vector for HA-tagged ZAPS or ZAP. Results are presented relative to *ACTB* expression (middle) or the activity of renilla luciferase (right). Left, immunoblot analysis of the expression of HA-tagged ZAPS and ZAP; far left lane, HEK293T cells transfected with control vector. (**c**) Quantitative RT-PCR analysis of ZAPS and ZAP mRNA in HEK293T cells stimulated for 0–12 h with 3pRNA (left) or IFN-α (500 U/ml; right); results are presented relative to expression at 0 h. (**d**) Quantitative RT-PCR analysis of ZAPS and ZAP mRNA induced by 3pRNA in human primary CD14$^+$ monocytes purified from peripheral blood mononuclear cells; results are presented relative to expression at 0 h. $^*P < 0.05$ and $^{**}P < 0.01$ (Student's *t*-test). Data are from one representative of at least two independent experiments (mean and s.d. of triplicate (**a**,**b**) or duplicate (**c**,**d**) samples).

PARP superfamily members also contribute to the host inflammatory and immune responses to viral infection. PARP-1 functions as a coactivator of NF-κB[27,28], a function for which the PARP enzymatic activity does not seem to be required. PARP-9 (BAL1), which lacks PARP activity[29] and is inducible by interferon-γ (IFN-γ), is able to increase the expression of interferon-stimulated genes[30], which suggests a putative role in the host defense against viral infection. However, the role of PARP superfamily members in the activation of innate signaling pathways mediated by PRRs such as RIG-I is not clearly understood.

Here we show that the shorter isoform of PARP-13 (ZAPS), rather than the full-length isoform (ZAP), was selectively induced by 3pRNA and functioned as a regulator of RIG-I-mediated signaling. Knockdown experiments show that ZAPS had a role in the induction of type I interferon genes in various human cell lines and human primary cells. Mechanistically, ZAPS directly associated with RIG-I in a ligand-dependent manner to efficiently promote the oligomerization of RIG-I, which resulted in much greater ATPase activity of RIG-I and subsequently enhancement of activation of the downstream IRF3 and NF-κB signaling pathways. Consistent with those results and data based on zinc-finger nuclease (ZFN)–mediated gene disruption, ZAPS strengthened the RIG-I-mediated induction of type I interferons and other inflammatory cytokines and inhibited viral replication after infection with RNA viruses that involve RIG-I, such as influenza virus and Newcastle disease virus (NDV). Our findings indicate that ZAPS has an important role as a potent stimulator of RIG-I signaling in the innate immune response to viral infection.

RESULTS

Contribution of PARPs to the interferon response

To investigate the role of the PARP-superfamily members in nucleic acid–induced innate immune responses, we chose to study some of the PARP superfamily members known to be involved in microbial infection, inflammation and immunity, including PARP-1, PARP-2, PARP-7, PARP-9, PARP-12 and PARP-13 (refs. 19,23,31–34). We then determined whether they were able to enhance the induction of IFN-β mRNA in HEK293T human embryonic kidney cells in response to stimulation with the following three different types of nucleic acids: 3pRNA; the synthetic double-stranded RNA polyinosinic-cytidylic acid (poly(rI:rC)); and the synthetic B-form double-stranded DNA poly(dA-dT)•poly(dA-dT) (poly(dA:dT)). Among the proteins tested, PARP-13 uniquely showed a substantial enhancement effect on the expression of IFN-β mRNA induced by stimulation with 3pRNA, poly(rI:rC) or poly(dA:dT) (**Fig. 1a**), each of which is known to activate the RIG-I-mediated pathway in HEK293T cells[9,10,35–37]. We also detected slightly more IFN-β mRNA expression in cells expressing PARP-1, PARP-2 and PARP-9. PARP-13 exists in at least two isoforms[22,26,38]. The amino-terminal 254-amino acid fragment of the rat PARP-13 homolog, which corresponds to the amino-terminal one-third portion of the shorter isoform of human PARP-13 protein, has been identified as rNZAP (rat N-terminal zinc finger antiviral protein)[20]. The expression of rNZAP results in specific decay of viral mRNA without any effect on the amount of mRNA derived from host cells[20,39]. However, the role of human PARP-13 in the induction of type I interferon remains unknown.

We first examined the role of the two PARP-13 isoforms in the induction of type I interferon by 3pRNA. Each isoform enhanced the induction of IFN-β mRNA and activation of the *IFNB* promoter after stimulation with 3pRNA (**Fig. 1b**). However, the shorter form of PARP-13 (isoform 2; ZAPS), which lacks the PARP domain, had a greater effect than did full-length PARP-13 (isoform 1; ZAP; **Fig. 1b**). This indicates that interferon induction does not necessarily require the PARP domain of PARP-13. Consistent with those observations, ZAPS mRNA was induced exclusively by stimulation with 3pRNA in both HEK293T cells and human primary CD14$^+$ monocytes purified

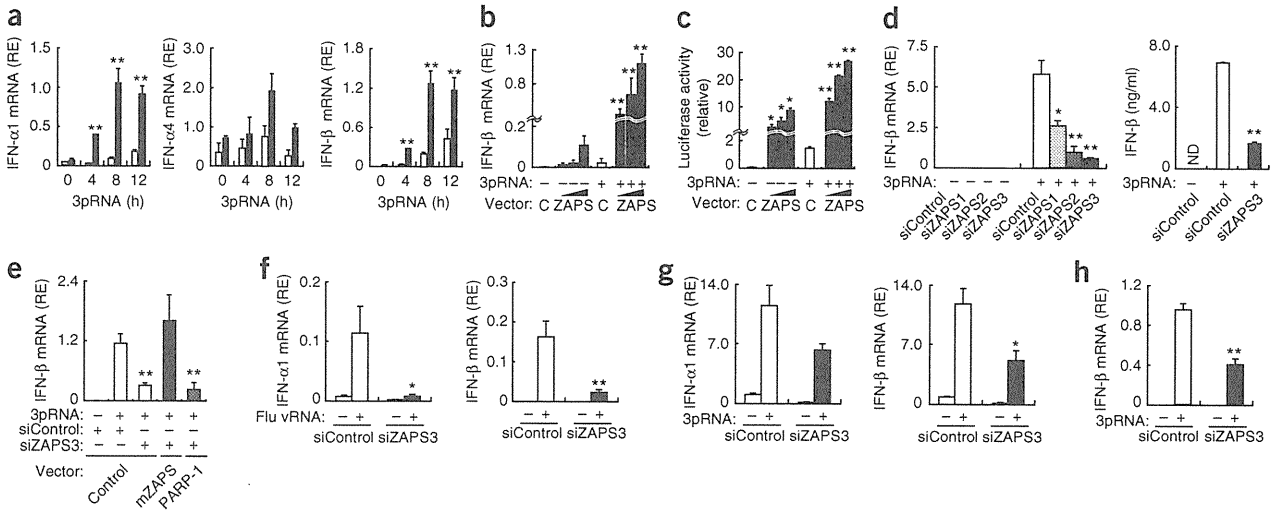

Figure 2 ZAPS is a potent stimulator of RIG-I-mediated type I interferon responses activated by 3pRNA. (**a**) Quantitative RT-PCR analysis of IFN-α1, IFN-α4 and IFN-β mRNA after 0–12 h of stimulation with 3pRNA in HEK293T cells transfected with control vector (open bars) or expression vector for ZAPS (filled bars). (**b**,**c**) Quantitative RT-PCR analysis of IFN-β mRNA after 8 h of 3pRNA stimulation (**b**) and luciferase activity of a p-125Luc reporter plasmid after 16 h of 3pRNA stimulation (**c**) in HEK293T cells transfected with increasing doses of control vector or ZAPS expression vector. (**d**) Quantitative RT-PCR analysis of IFN-β mRNA after 8 h of 3pRNA stimulation (left) and ELISA of IFN-β 24 h after 3pRNA stimulation (right) in HEK293T cells transfected with control siRNA (siControl) or with siZAPS1, siZAPS2 or siZAPS3. ND, not detected. (**e**) Quantitative RT-PCR analysis of IFN-β mRNA after 8 h of 3pRNA stimulation in HEK293T cells cotransfected with control vector or expression vector for mouse ZAPS (mZAPS) or PARP-1, plus siControl or siZAPS3. (**f**) Quantitative RT-PCR analysis of IFN-α1 and IFN-β mRNA after 8 h of stimulation with viral RNA derived from influenza virus (Flu vRNA) in A549 cells treated with siControl or siZAPS3. (**g**,**h**) Quantitative RT-PCR analysis of type I interferon mRNA after 8 h of stimulation with 3pRNA in human primary $CD14^+$ monocytes (**g**) and MRC-5 fibroblasts (**h**) treated for 48 h with siControl or siZAPS3. RT-PCR results (**a**,**b**,**d**–**h**) are presented relative to *ACTB* expression; luciferase results are presented relative to the activity of renilla luciferase (**c**). $^*P < 0.05$ and $^{**}P < 0.01$ (Student's *t*-test). Data are from one representative of at least two independent experiments (mean and s.d. of triplicate (**a**–**f**,**h**) or duplicate (**g**) samples).

from peripheral blood mononuclear cells, whereas full-length ZAP was constitutively expressed but was barely induced (**Fig. 1c**, left, **d**). The promoter region of the gene encoding ZAP (*ZC3HAV1*) contains interferon-stimulated response elements and IRF-binding elements[40]. We investigated whether expression of ZAPS and ZAP is regulated by similar mechanisms. Treatment with IFN-α resulted in the induction of ZAPS but not of full-length ZAP (**Fig. 1c**, right). These data suggest that the mechanism of ZAPS induction differs from that of ZAP induction and indicate a distinct role for ZAPS as a regulator of innate immunity. Therefore, we focused on the function of ZAPS in RIG-I signaling.

ZAPS enhances RIG-I-mediated production of type I interferon

Next we examined the effect of ZAPS in RIG-I-mediated induction of type I interferon. Expression of ZAPS in HEK293T cells markedly enhanced the 3pRNA-induced expression of IFN-α1 and IFN-α4 mRNA as well as IFN-β mRNA (**Fig. 2a**). The enhancement of IFN-β mRNA induction correlated positively with ZAPS overexpression (**Fig. 2b**). Consistent with that result, 3pRNA induced activation of the *IFNB* promoter in a manner dependent on the amount of ZAPS expression in HEK293T cells (**Fig. 2c** and **Supplementary Fig. 1a**). We observed activation of genes encoding type I interferons and interferon-related genes even in the absence of 3pRNA stimulation (**Fig. 2b**,**c** and **Supplementary Fig. 1b**). In contrast, ZAPS did not have a positive effect on a luciferase reporter responsive to the transcription factor E2F or driven by the serum response element (**Supplementary Fig. 1c**) or on the induction of E2F target genes and serum response element–dependent genes (**Supplementary Fig. 1b**).

To further evaluate the contribution of ZAPS to the RIG-I signaling, we used an RNA-mediated interference approach. Notably, each small interfering RNA (siRNA) targeting a different site of ZAPS mRNA (siZAPS1, siZAPS2 and siZAPS3) knocked down the expression of endogenous ZAPS protein and ZAPS mRNA (**Supplementary Fig. 2a**,**b**), which resulted in significant suppression of 3pRNA-induced expression of IFN-β mRNA in HEK293T cells (**Fig. 2d**, left). Knockdown with siZAPS3 also resulted in significant inhibition of the production of IFN-β protein in response to 3pRNA stimulation, as assessed by enzyme-linked immunosorbent assay (ELISA; **Fig. 2d**, right). Furthermore, the knockdown effect of siZAPS3 could be 'rescued' by the expression of mouse ZAPS that does not carry the target sequence for siZAPS3 (**Fig. 2e**) but not by the expression of another PARP superfamily member, PARP-1, which did not significantly affect 3pRNA-induced expression of IFN-β mRNA (**Figs. 1a** and **2e**). We also examined the effect of siZAPS3 knockdown in the following additional cell types: the A549 human lung epithelial adenocarcinoma cell line, the HeLa cervical cancer cell line and the THP-1 acute monocytic leukemia cell line. The induction of IFN-α and IFN-β mRNA in response to 3pRNA or to viral RNA derived from influenza virus was abrogated by knockdown of endogenous ZAPS protein with siZAPS3 (**Fig. 2f**, **Supplementary Fig. 2c**,**d** and data not shown). Furthermore, the type I interferon response to 3pRNA was significantly suppressed by knockdown of ZAPS in human primary $CD14^+$ monocytes (**Fig. 2g**) and fibroblasts (**Fig. 2h**), which indicates the physiological importance of ZAPS in human cells. These results suggest that ZAPS is a potent stimulator of the RIG-I-mediated type I interferon response.

ZAPS facilitates NF-κB and IRF3 signaling

We next investigated whether ZAPS can enhance NF-κB and IRF3 signaling downstream of RIG-I. The induction of genes encoding other

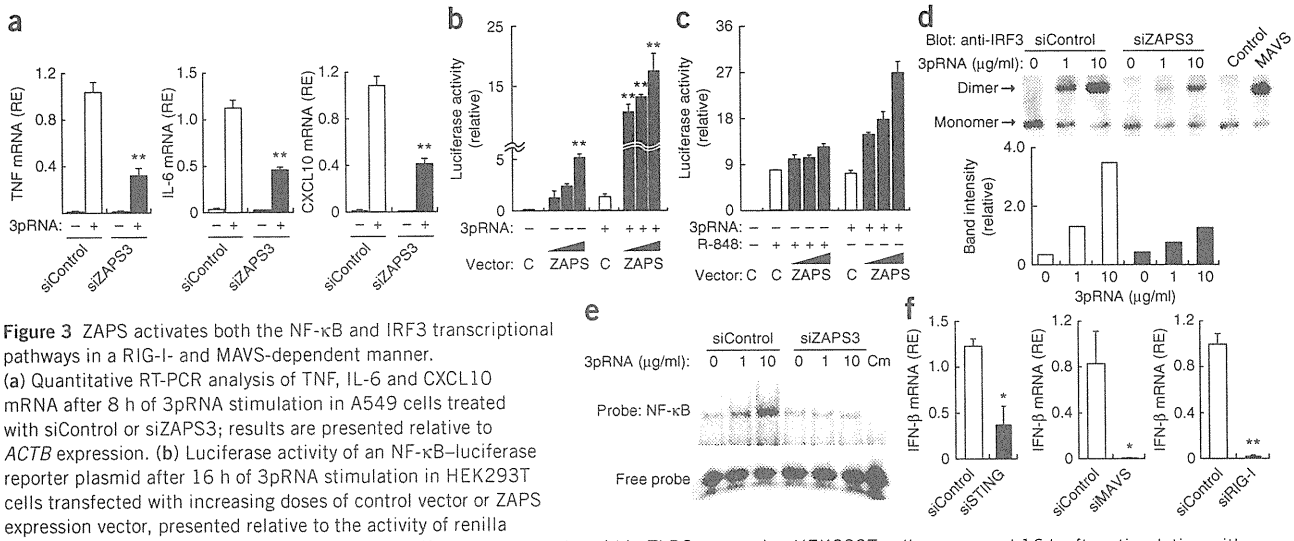

Figure 3 ZAPS activates both the NF-κB and IRF3 transcriptional pathways in a RIG-I- and MAVS-dependent manner. (**a**) Quantitative RT-PCR analysis of TNF, IL-6 and CXCL10 mRNA after 8 h of 3pRNA stimulation in A549 cells treated with siControl or siZAPS3; results are presented relative to *ACTB* expression. (**b**) Luciferase activity of an NF-κB–luciferase reporter plasmid after 16 h of 3pRNA stimulation in HEK293T cells transfected with increasing doses of control vector or ZAPS expression vector, presented relative to the activity of renilla luciferase. (**c**) Luciferase activity of an NF-κB–luciferase reporter plasmid in TLR8-expressing HEK293T cells, measured 16 h after stimulation with 3pRNA or R-848, presented relative to the activity of renilla luciferase. (**d**) Native PAGE and immunoblot analysis (top) of 3pRNA-induced dimerization of endogenous IRF3 in HEK293T cells treated with siControl (open bars) or siZAPS3 (filled bars); right, lysates from HEK293T cells transfected with control or MAVS expression vector (negative or positive control, respectively). Below, band intensity of the IRF3 dimer relative to that of the IRF3 monomer, assessed by densitometry. (**e**) Electrophoretic mobility-shift assay of NF-κB activation induced by 3pRNA stimulation in HEK293T cells treated with siControl or siZAPS3; far right (Cm), competition by cold probe. (**f**) Quantitative RT-PCR analysis of IFN-β mRNA 48 h after cotransfection of HEK293T cells with siControl or siRNA targeting STING, MAVS or RIG-I, along with ZAPS expression vector; results are presented relative to *ACTB* expression. $^*P < 0.05$ and $^{**}P < 0.01$ (Student's *t*-test). Data are from one representative of at least two independent experiments (mean and s.d. of triplicate (**a–c**) or duplicate (**f**) samples).

cytokines, such as tumor necrosis factor (TNF), interleukin 6 (IL-6) and the chemokine CXCL10, in response to stimulation with 3pRNA was diminished in A549 cells in which ZAPS was knocked down (**Fig. 3a**). This suggests that ZAPS also activates the NF-κB pathway, another important signaling branch of the RIG-I-mediated pathway. Consistent with that idea, ZAPS overexpression in HEK293T cells induced robust activation (13-fold) of an NF-κB-responsive promoter after stimulation with 3pRNA (**Fig. 3b**). However, ZAPS had a lower activating effect on the NF-κB-responsive promoter after stimulation of TLR8 by the synthetic imidazoquinoline resiquimod (R-848; **Fig. 3c**). Dimerization of IRF3 (a transcription factor essential for RIG-I-mediated production of type I interferon) induced by 3pRNA was much lower in HEK293T cells pretreated with siZAPS3 (**Fig. 3d**). In addition, electrophoretic mobility-shift assay showed that NF-κB activation in response to stimulation with 3pRNA was inhibited in HEK293T cells pretreated with siZAPS3 (**Fig. 3e**). Collectively, these data indicate that ZAPS may be an essential component of the RIG-I-mediated signaling pathway, affecting activation of both the IRF3- and NF-κB-activation pathways.

Activation of RIG-I transmits signals to the adaptor protein MAVS, which leads to the activation of TBK1, one of the IRF3 kinases[6,7]. STING (also known as TMEM173, MITA, ERIS or MPYS), a signaling mediator possibly situated downstream of MAVS, can activate both the NF-κB and IRF3 pathways[15,41]. As TBK1 can activate only the IRF pathway after stimulation with cytosolic RNA[6,7,15], we speculated that ZAPS may function upstream of TBK1. Indeed, the expression of IFN-β mRNA induced by exogenous expression of ZAPS in HEK293T cells was abolished by siRNA-mediated downregulation of TBK1 (**Supplementary Fig. 3**). Notably, ablation of not only STING or MAVS but also RIG-I in HEK293T cells, achieved by RNA-mediated interference, inhibited ZAPS-mediated expression of IFN-β mRNA (**Fig. 3f**). These results suggest a role for ZAPS as a proximal regulator of RIG-I-mediated signaling.

Interaction of ZAPS with RIG-I

To gain insight into how ZAPS functions as a potentiator of RIG-I activation, we determined whether ZAPS interacts with RIG-I. Confocal analysis of HeLa cells transfected with yellow fluorescent protein (YFP)-tagged ZAPS and Flag-tagged RIG-I showed that these two proteins localized together with each other mainly in the cytoplasm 4 h after stimulation with 3pRNA (**Fig. 4a**). In addition, we detected a fluorescence resonance energy transfer (FRET) signal in the cytoplasmic perinuclear space after stimulation with 3pRNA (**Fig. 4b**). These results indicate that ZAPS interacts directly with RIG-I after ligand stimulation. In an immunoprecipitation assay, the interaction between ZAPS and RIG-I recombinant proteins produced in *Escherichia coli* was enhanced in the presence of viral RNA (**Supplementary Fig. 4a**). In HEK293T cells expressing hemagglutinin-tagged (HA-tagged) ZAPS and Flag-tagged RIG-I, the interaction between the two proteins was enhanced after stimulation with 3pRNA or viral RNA (**Fig. 4c**, left, and **Supplementary Fig. 4b**), and we similarly observed such a ZAPS–RIG-I interaction after infection with NDV (**Fig. 4c**, middle). We confirmed that endogenous ZAPS protein associated with endogenous RIG-I in MRC-5 human fibroblasts and A549 cells (**Fig. 4c**, right, and **Supplementary Fig. 4c**).

We also determined that the carboxy-terminal region of RIG-I (amino acids 218–925) but not its CARDs (amino acids 1–284) was required for interaction with ZAPS (**Fig. 4d**). In addition, the carboxy-terminal region of RIG-I, but not full-length RIG-I, 'preferentially' interacted with ZAPS even in the absence of 3pRNA stimulation (**Fig. 4d**), which suggested that the activation-induced conformational change of RIG-I may be necessary for its interaction with ZAPS. However, ZAPS did not bind to either the helicase domain or the carboxy-terminal domain of RIG-I alone (**Supplementary Fig. 4d**). Both of those domains seemed to be required for the interaction with ZAPS. In contrast, full-length ZAPS coimmunoprecipitated with the carboxy-terminal region of RIG-I, but a truncated ZAPS lacking all

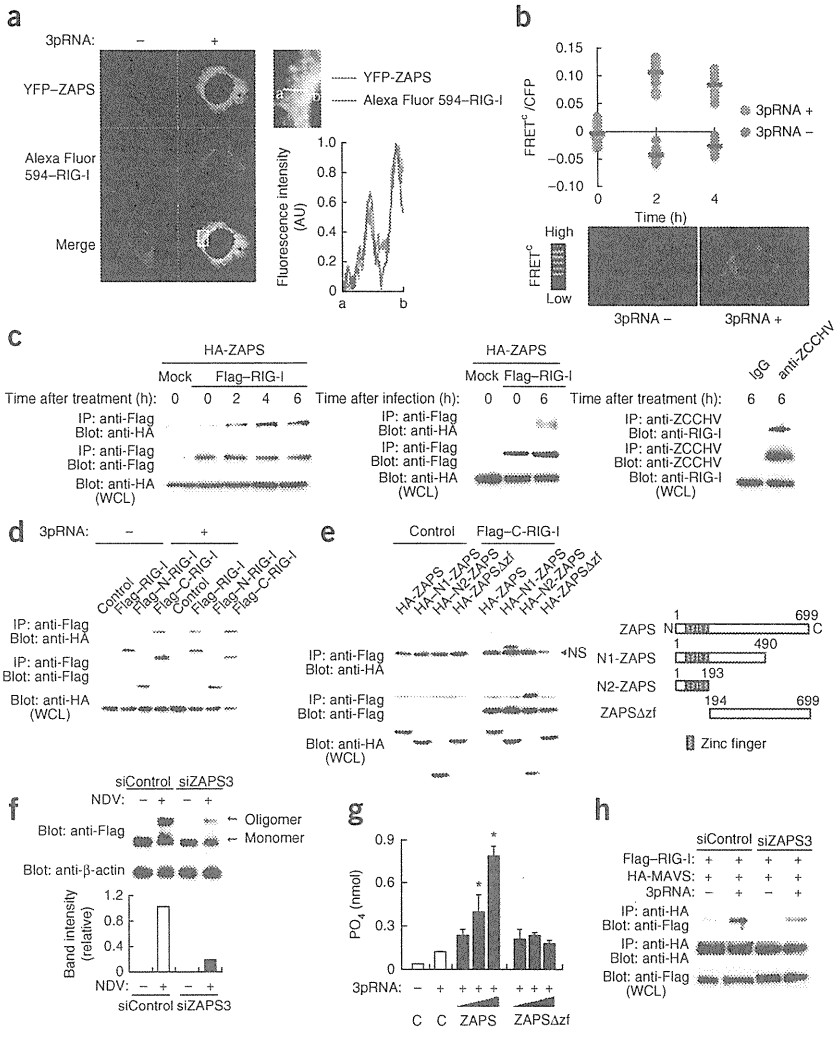

Figure 4 ZAPS interacts with RIG-I to positively modulate the RIG-I activity. (**a**) Fluorescence confocal microscopy of HeLa cells cotransfected with YFP-tagged ZAPS and Flag-tagged RIG-I (secondarily visualized with Alexa Fluor 594), before (–) and after (+) 4 h of 3pRNA stimulation. Top right, enlargement of area outlined at left (bottom row); below, line scan of fluorescence intensity of the white line (**a**–**b**) above. AU, arbitrary units. Original magnification, ×60. (**b**) Intermolecular FRET (top) of the interaction between YFP-tagged ZAPS and cyan fluorescent protein (CFP)-tagged RIG-I in HeLa cells with (+) or without (–) 3pRNA stimulation, presented as the ratio of corrected FRET ($FRET^c$) to CFP (small horizontal bars, mean). Below, fluorescence images of corrected FRET (pseudocolor mode). (**c**) Immunoprecipitation (IP; with anti-Flag) of HA-tagged ZAPS together with Flag-tagged RIG-I in lysates of HEK293T cells after mock treatment or treatment with 3pRNA (left) or infection with NDV (middle), followed by immunoblot analysis with anti-HA or anti-Flag. Right, coimmunoprecipitation of endogenous ZAPS and RIG-I in MRC-5 cells after 6 h of stimulation with 3pRNA; anti-ZCCHV, rabbit polyclonal antibody that can detect ZAPS as well as ZAP. Bottom, immunoblot analysis of whole-cell lysates (WCL) with anti-HA (left, middle) or anti-RIG-I (right). (**d**) Interaction of HA-tagged ZAPS with Flag-tagged full-length RIG-I or deletion mutants of RIG-I in HEK293T cells after 6 h of stimulation with 3pRNA, assessed as described in **c**. C-RIG-I, carboxy-terminal region of RIG-I; N-RIG-I, amino-terminal CARDs of RIG-I. (**e**) Interaction of Flag-tagged carboxy-terminal region of RIG-I with HA-tagged ZAPS or its mutants (N1-ZAPS, N2-ZAPS or ZAPSΔzf; right) in HEK293T cells, analyzed as described in **c**. (**f**) Native PAGE and immunoblot analysis (top) of the oligomerization of Flag-tagged RIG-I induced by NDV infection (16 h) in HEK293T cells treated with siControl or siZAPS3. Below, band intensity of the RIG-I oligomer relative to that of the RIG-I monomer. (**g**) ATPase activity of recombinant RIG-I protein after the addition of 3pRNA in the presence of increasing doses of recombinant glutathione *S*-transferase–tagged ZAPS or ZAPSΔzf. $^*P < 0.01$ (Student's *t*-test). (**h**) Association of Flag-tagged RIG-I with HA-tagged MAVS after 6 h of 3pRNA stimulation in HEK293T cells treated with siControl or siZAPS3, assessed as described in **c**. Data are from one representative of at least two independent experiments (mean and s.d. of triplicate samples in **g**).

four of the zinc fingers in its amino-terminal region (ZAPSΔzf) did not (**Fig. 4e**), which suggested that ZAPS binds to RIG-I via the zinc fingers. In addition, surface plasmon resonance–based analysis of recombinant ZAPS and RIG-I showed that ZAPS interact with RIG-I even in the absence of 3pRNA, with an affinity in the nanomolar range (dissociation constant, 116 nM; **Supplementary Fig. 4e**), but it failed to enhance the binding of RIG-I to 3pRNA (data not shown).

We next determined whether ZAPS is involved in RIG-I activation. We first examined the involvement of ZAPS in 3pRNA- or virus-induced RIG-I dimerization or oligomerization, which is important in activation of the downstream signaling pathway for interferon production[42–44]. The formation of RIG-I oligomers induced by 3pRNA or NDV was diminished in HEK293T cells with downregulated expression of ZAPS (**Fig. 4f** and **Supplementary Fig. 4f**). These data suggest that ZAPS regulates RIG-I oligomerization for the subsequent robust activation of RIG-I signaling. *In vitro* biochemical analysis demonstrated that the 3pRNA-induced ATPase activity of purified recombinant RIG-I was much greater in the presence of recombinant ZAPS but not in the presence of ZAPSΔzf (**Fig. 4g**). We further found that the association of RIG-I with its adaptor MAVS was substantially attenuated in HEK293T cells treated with siZAPS3 (**Fig. 4h**). These findings suggest that ZAPS associates with RIG-I to positively modulate the oligomerization and activation of RIG-I.

Role of ZAPS in infection with RNA viruses

To further evaluate the function of ZAPS in RIG-I-mediated antiviral responses, we infected A549 cells with influenza virus, which activates RIG-I-mediated innate signaling[10,45]. We found that siRNA-mediated knockdown of ZAPS expression impaired the induction of IFN-β and IFN-α1 mRNA (**Fig. 5a** and **Supplementary Fig. 5a**) and IFN-β protein (**Fig. 5b**) in response to infection with influenza virus (strains A/X-31 (H3N2) and A/Aichi/2/1968 (H3N2)). The induction of IL-6, TNF and CXCL10 was also lower (**Fig. 5a**). Expression of the viral nucleoprotein was not affected by siRNA-mediated knockdown of ZAPS in the early phase of infection (**Supplementary Fig. 5b**). However, we detected approximately sevenfold more of the viral nucleoprotein gene in siZAPS3-treated A549 cells at 72 h after infection with influenza virus (A/X-31) than in A549 cells

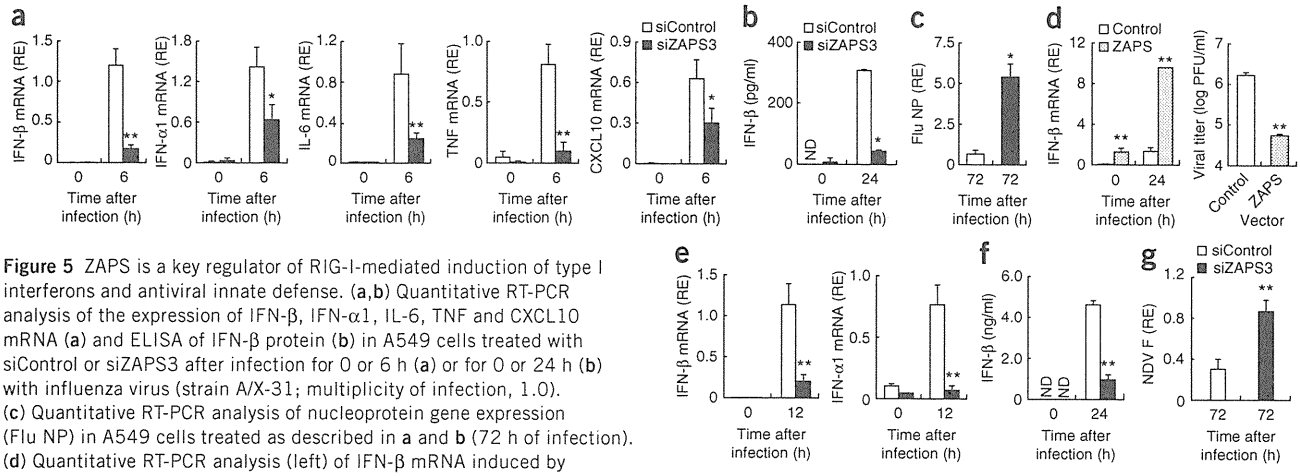

Figure 5 ZAPS is a key regulator of RIG-I-mediated induction of type I interferons and antiviral innate defense. (**a**,**b**) Quantitative RT-PCR analysis of the expression of IFN-β, IFN-α1, IL-6, TNF and CXCL10 mRNA (**a**) and ELISA of IFN-β protein (**b**) in A549 cells treated with siControl or siZAPS3 after infection for 0 or 6 h (**a**) or for 0 or 24 h (**b**) with influenza virus (strain A/X-31; multiplicity of infection, 1.0). (**c**) Quantitative RT-PCR analysis of nucleoprotein gene expression (Flu NP) in A549 cells treated as described in **a** and **b** (72 h of infection). (**d**) Quantitative RT-PCR analysis (left) of IFN-β mRNA induced by infection with influenza virus (multiplicity of infection, 1.0) in HEK293T cells transfected with control or ZAPS expression vector. Right, plaque-forming assay of viral titers after 48 h of infection (PFU, plaque-forming units). (**e**,**f**) Quantitative RT-PCR analysis of the expression of IFN-β and IFN-α1 mRNA (**e**) and ELISA of IFN-β (**f**) in A549 cells treated with siControl or siZAPS3 after infection for 0 or 12 h (**e**) or for 0 or 24 h (**f**) with NDV. (**g**) Quantitative RT-PCR analysis of the expression of the gene encoding NDV F protein in cells treated as described in **e** and **f** (72 h of infection). RT-PCR results (**a**,**c**–**e**,**g**) are presented relative to the expression of *GAPDH* (encoding glyceraldehyde phosphate dehydrogenase). $^*P < 0.05$ and $^{**}P < 0.01$ (Student's *t*-test). Data are from one representative of at least two independent experiments (mean and s.d. of triplicate (**a**–**c**,**e**–**g**) or duplicate (**d**) samples).

treated with control siRNA (**Fig. 5c**). Moreover, exogenous expression of ZAPS in HEK293T cells resulted in increased induction of IFN-β mRNA after infection with influenza virus, accompanied by considerable suppression of viral replication (**Fig. 5d**). We also obtained similar results after infection with NDV (**Fig. 5e–g**), another single-stranded RNA virus also known to induce type I interferon responses via RIG-I (refs. 4,45). Our data suggest that ZAPS exerts its antiviral activity mainly by interactions with the RIG-I-mediated type I interferon pathway (**Supplementary Fig. 5c**), although the possibility of an indirect effect on viral replication cannot be completely ruled out.

ZAPS mediates RIG-I activation in human cells

To further confirm the critical role of ZAPS in human cells, we used a ZFN approach[46–48] for site-specific disruption at the targeted site in exon 3 of *ZC3HAV1*, the gene encoding endogenous PARP-13 (**Fig. 6a**). We established two *ZC3HAV1*-knockout clones derived from multiploid HEK293T cells. Genome sequence analysis showed that clone 32 and clone 89 had the following distinct mutations in isoform 2 of *ZC3HAV1* (GenBank accession number NM_024625.3): clone 32, c.1023_1047del25insGTT, c.1027_1046del20, c.1031_1032insATCCA and c.1033_1034insCAATC; clone 89, c.1035_1036insTCCA, c.1023_1047del25insGTT and c.1027_1046del20. All these mutations abolished the expression of functional protein (**Fig. 6b**). In these two genetically distinct knockout clones, NDV infection failed to induce the expression of mRNA for IFN-β and other cytokines (**Fig. 6c**). IFN-β expression induced by 3pRNA was similarly inhibited in both clone 32 and clone 89, and this phenotype was 'rescued' by exogenous expression of ZAPS (**Fig. 6d**). These results suggest that ZAPS has a crucial role in RIG-I-mediated gene induction.

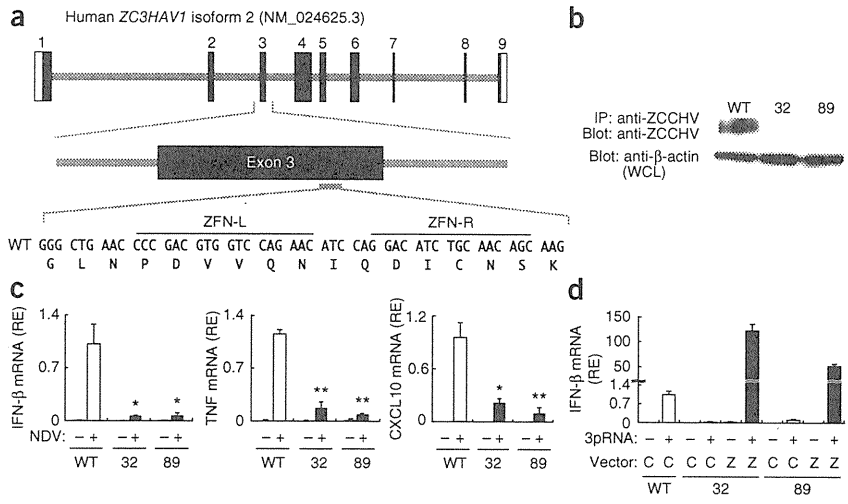

Figure 6 Crucial role for ZAPS in the induction of cytokine genes by NDV infection. (**a**) Strategy for site-specific gene disruption for the generation of human *ZC3HAV1*-knockout cells, showing the ZFN-targeting site in the exon 3; ZFN-L and ZFN-R are recognition sites of the designed ZFN pairs. (**b**) Immunoprecipitation and immunoblot analysis of ZAPS expression in parental HEK293T cells (WT) and *ZC3HAV1*-knockout clones 32 and 89, probed with anti-ZCCHV. Bottom, immunoblot analysis of whole-cell lysates (loading control). (**c**) Quantitative RT-PCR analysis of the induction of IFN-β, TNF and CXCL10 mRNA in response to NDV infection (8 h) in parental HEK293T cells (open bars) and *ZC3HAV1*-knockout clones 32 and 89 (filled bars). (**d**) Quantitative RT-PCR analysis of IFN-β mRNA after 8 h of 3pRNA stimulation in parental HEK293T cells and *ZC3HAV1*-knockout clones 32 and 89, transfected with control vector (C; open bars) or ZAPS expression vector (Z; filled bars). RT-PCR results are presented relative to *ACTB* expression. $^*P < 0.05$ and $^{**}P < 0.01$ (Student's *t*-test). Data are from one representative of at least two independent experiments (mean and s.d. of triplicate samples in **c**,**d**).

DISCUSSION

The PARP superfamily has important roles in many biological and pathological processes. Some members of the PARP superfamily are known to directly regulate viral gene expression and replication. However, the role of the PARP superfamily in host immune responses mediated by innate sensors has remained unknown. In this study we have demonstrated that PARP-13 was a regulator of RIG-I-mediated antiviral signaling in human cells. We also found that ZAPS, the shorter isoform of PARP-13 (ZAP), was selectively upregulated by treatment with 3pRNA, possibly through type I interferon signaling. In this context, it has been speculated that ZAPS may act as a positive feedback regulator in RIG-I-mediated induction of type I interferon genes. Consistent with that scenario, the promoter of the gene encoding ZAP (and ZAPS) contains interferon-stimulated response elements and IRF-binding elements. How each isoform is regulated differently remains unclear.

Activation of RIG-I by 3pRNA leads to its association with MAVS and activation of the cytosolic protein kinases IKK and TBK1, which in turn activate the transcription factors NF-κB and IRF3 or IRF7, respectively[6,15]. RIG-I activation after ligand binding is thought to be a multistep process that includes the activation of its ATPase activity, conformational changes and oligomerization[42,43]. Our data have demonstrated that ZAPS interacted with RIG-I after stimulation with 3pRNA and potently enhanced the ATPase activity and oligomerization of RIG-I, possibly by stabilizing the RNA–RIG-I complex, although the underlying mechanism needs to be investigated further. Consistent with that, ZAPS robustly enhanced downstream gene-expression programs mediated by RIG-I–MAVS, including those of genes encoding type I interferons and proinflammatory cytokines. However, our results also indicated that ZAPS expression alone slightly enhanced the expression of IFN-β mRNA and activation of the *IFNB* promoter independently of any ligand or other stimuli. Consistent with those data, we detected the ZAPS–RIG-I interaction before stimulation, although it was very weak. This disconnection of ligand dependence suggested that the ZAPS–RIG-I interaction was sufficient to promote small amounts of signaling but that the overall signaling program was most efficiently triggered by the binding of ligand to RIG-I in addition to its activation by ZAPS.

Lys63 (K63)-linked polyubiquitination of RIG-I mediated by the ubiquitin ligase TRIM25 represents another important modification that links RIG-I activation to MAVS[17]. Other mediators of protein modification, such as ISG15, RNF125, CYLD and Riplet (REUL), also have a regulatory role in RIG-I activation[49–52]. In addition, unanchored K63-ubiquitin chains, which are not conjugated to any target protein, positively regulate RNA-triggered activation of RIG-I through their binding to RIG-I CARDs[16]. Our results support the idea that ZAPS functions as a RIG-I regulator upstream of the ubiquitin-mediated regulatory mechanisms, although further analyses are needed to clarify whether ZAPS participates in the ubiquitination of RIG-I.

AT-rich double-stranded DNA can be transcribed into 3pRNA by DNA-dependent RNA polymerase III, resulting in activation of RIG-I and production of type I interferon and activation of the NF-κB pathway[36,37]. In this context, it can be presumed that ZAPS may also enhance cytosolic DNA–triggered cytokine induction through its positive regulation of RIG-I pathway. That possibility was supported by our preliminary observation that poly(dA:dT)-triggered induction of type I interferons was significantly abolished in HEK293T cells treated with siRNA targeting ZAPS ($P < 0.01$; S.H., S.S., H.Y. and A.T., unpublished data).

Our data showing that ZAPS was critically involved in antiviral innate immune responses to influenza virus and NDV raised the possibility that ZAPS may have an important role in host defense against many other viruses known to activate RIG-I signaling, such as Sendai virus, hepatitis C virus and Japanese encephalitis virus[45,53]. Further investigation of the role of ZAPS in other virus-activated, PRR-mediated innate signaling is needed. In addition to the important role of ZAPS in RIG-I-mediated responses in human cells, we have preliminary data showing a function for ZAPS in several mouse cell lines (data not shown), although this remains to be further investigated.

ZAP has a role in the decay of mRNA derived from certain viral subsets[20,26,39]. Our data showing that ZAPS facilitated the activation of innate antiviral mechanisms indicate that ZAPS might exert a dual mode of defense activity against viral infection. These activities might be regulated differently through the ability of ZAPS to bind two distinct RNA helicases: RIG-I for the activation of host innate immune response, and p72 for the degradation of viral RNA[25,26]. How these activities are regulated remains to be clarified. In addition, because of its dual antiviral function, activation of ZAPS could provide a therapeutic application aimed at enhancing antiviral responses.

METHODS

Methods and any associated references are available in the online version of the paper at http://www.nature.com/natureimmunology/.

Note: Supplementary information is available on the Nature Immunology website.

ACKNOWLEDGMENTS

We thank T. Fujita (Kyoto University) for the luciferase reporter plasmids p-55C1BLuc and p-125Luc; J. Miyazaki (Osaka University) for the pCAGGS vector; A. Miyawaki (RIKEN) for the Venus vector; H. Kida (Hokkaido University) for NDV; A. Iwai, H. Higashi and J. Hamada for technical help; M. Yamane for the purification of human primary $CD14^+$ monocytes; and S. Tamura and T. Moriyama for advice on recombinant protein purification. Supported by the Ministry of Education, Culture, Sports, Science and Technology of Japan (Grant-in-Aid for Young Scientists (A) to S.H., Young Scientists (S) to A.T.) and Scientific Research in Priority Areas (A.T.), IRYO HOJIN SHADAN JIKOKAI (H. Tanaka & N. Takayanagi) (A.T.), the Astellas Foundation for Research on Metabolic Disorders (A.T.), the Kanae Foundation for the Promotion of Medical Science (A.T.), the Kato Memorial Bioscience Foundation (A.T.) and the Yasuda Medical Foundation (A.T.).

AUTHOR CONTRIBUTIONS

S.H., S.S., H.Y., T.K., C.K., F.K., S.G., S.K., T.Y., M.K., M.S., J.T., M.A. and M.I. planned studies, did experiments and analyzed data; D.F. and T. Miyazaki contributed to viral infection experiments and helped with data analyses; T. Mizutani and Y.O. did fluorescence microscopy experiments and FRET analysis; and A.T. supervised the project, designed experiments and wrote the manuscript with comments from the coauthors.

COMPETING FINANCIAL INTERESTS

The authors declare no competing financial interests.

Published online at http://www.nature.com/natureimmunology/.
Reprints and permissions information is available online at http://npg.nature.com/reprintsandpermissions/.

1. Takeuchi, O. & Akira, S. Pattern recognition receptors and inflammation. *Cell* **140**, 805–820 (2010).
2. Takaoka, A. & Taniguchi, T. Cytosolic DNA recognition for triggering innate immune responses. *Adv. Drug Deliv. Rev.* **60**, 847–857 (2008).
3. Katze, M., Fornek, J., Palermo, R., Walters, K. & Korth, M. Innate immune modulation by RNA viruses: emerging insights from functional genomics. *Nat. Rev. Immunol.* **8**, 644–654 (2008).
4. Yoneyama, M. *et al.* The RNA helicase RIG-I has an essential function in double-stranded RNA-induced innate antiviral responses. *Nat. Immunol.* **5**, 730–737 (2004).
5. Yoneyama, M. *et al.* Shared and unique functions of the DExD/H-box helicases RIG-I, MDA5, and LGP2 in antiviral innate immunity. *J. Immunol.* **175**, 2851–2858 (2005).
6. Yoneyama, M. & Fujita, T. RNA recognition and signal transduction by RIG-I-like receptors. *Immunol. Rev.* **227**, 54–65 (2009).

7. Takeuchi, O. & Akira, S. Innate immunity to virus infection. *Immunol. Rev.* **227**, 75–86 (2009).
8. Rehwinkel, J. & Reis e Sousa, C. RIGorous detection: exposing virus through RNA sensing. *Science* **327**, 284–286 (2010).
9. Hornung, V. *et al.* 5′-Triphosphate RNA is the ligand for RIG-I. *Science* **314**, 994–997 (2006).
10. Pichlmair, A. *et al.* RIG-I-mediated antiviral responses to single-stranded RNA bearing 5′-phosphates. *Science* **314**, 997–1001 (2006).
11. Kawai, T. *et al.* IPS-1, an adaptor triggering RIG-I- and Mda5-mediated type I interferon induction. *Nat. Immunol.* **6**, 981–988 (2005).
12. Meylan, E. *et al.* Cardif is an adaptor protein in the RIG-I antiviral pathway and is targeted by hepatitis C virus. *Nature* **437**, 1167–1172 (2005).
13. Seth, R.B., Sun, L., Ea, C.K. & Chen, Z.J. Identification and characterization of MAVS, a mitochondrial antiviral signaling protein that activates NF-κB and IRF 3. *Cell* **122**, 669–682 (2005).
14. Xu, L. *et al.* VISA is an adapter protein required for virus-triggered IFN-β signaling. *Mol. Cell* **19**, 727–740 (2005).
15. Nakhaei, P., Genin, P., Civas, A. & Hiscott, J. RIG-I-like receptors: sensing and responding to RNA virus infection. *Semin. Immunol.* **21**, 215–222 (2009).
16. Zeng, W. *et al.* Reconstitution of the RIG-I pathway reveals a signaling role of unanchored polyubiquitin chains in innate immunity. *Cell* **141**, 315–330 (2010).
17. Gack, M. *et al.* TRIM25 RING-finger E3 ubiquitin ligase is essential for RIG-I-mediated antiviral activity. *Nature* **446**, 916–920 (2007).
18. Cui, J. *et al.* NLRC5 negatively regulates the NF-κB and type I interferon signaling pathways. *Cell* **141**, 483–496 (2010).
19. Hakme, A., Wong, H.K., Dantzer, F. & Schreiber, V. The expanding field of poly(ADP-ribosyl)ation reactions. 'Protein Modifications: Beyond the Usual Suspects' Review Series. *EMBO Rep.* **9**, 1094–1100 (2008).
20. Gao, G., Guo, X. & Goff, S.P. Inhibition of retroviral RNA production by ZAP, a CCCH-type zinc finger protein. *Science* **297**, 1703–1706 (2002).
21. Hassa, P.O. & Hottiger, M.O. The diverse biological roles of mammalian PARPS, a small but powerful family of poly-ADP-ribose polymerases. *Front. Biosci.* **13**, 3046–3082 (2008).
22. Schreiber, V., Dantzer, F., Ame, J.C. & de Murcia, G. Poly(ADP-ribose): novel functions for an old molecule. *Nat. Rev. Mol. Cell Biol.* **7**, 517–528 (2006).
23. Tempera, I. *et al.* Regulation of Epstein-Barr virus OriP replication by poly(ADP-ribose) polymerase 1. *J. Virol.* **84**, 4988–4997 (2010).
24. Ohsaki, E. *et al.* Poly(ADP-ribose) polymerase 1 binds to Kaposi's sarcoma-associated herpesvirus (KSHV) terminal repeat sequence and modulates KSHV replication in latency. *J. Virol.* **78**, 9936–9946 (2004).
25. Chen, G., Guo, X., Lv, F., Xu, Y. & Gao, G. p72 DEAD box RNA helicase is required for optimal function of the zinc-finger antiviral protein. *Proc. Natl. Acad. Sci. USA* **105**, 4352–4357 (2008).
26. Zhu, Y. & Gao, G. ZAP-mediated mRNA degradation. *RNA Biol.* **5**, 65–67 (2008).
27. Hassa, P., Buerki, C., Lombardi, C., Imhof, R. & Hottiger, M. Transcriptional coactivation of nuclear factor-κB-dependent gene expression by p300 is regulated by poly(ADP)-ribose polymerase-1. *J. Biol. Chem.* **278**, 45145–45153 (2003).
28. Oliver, F. *et al.* Resistance to endotoxic shock as a consequence of defective NF-κB activation in poly (ADP-ribose) polymerase-1 deficient mice. *EMBO J.* **18**, 4446–4454 (1999).
29. Aguiar, R., Takeyama, K., He, C., Kreinbrink, K. & Shipp, M. B-aggressive lymphoma family proteins have unique domains that modulate transcription and exhibit poly(ADP-ribose) polymerase activity. *J. Biol. Chem.* **280**, 33756–33765 (2005).
30. Juszczynski, P. *et al.* BAL1 and BBAP are regulated by a γ interferon-responsive bidirectional promoter and are overexpressed in diffuse large B-cell lymphomas with a prominent inflammatory infiltrate. *Mol. Cell. Biol.* **26**, 5348–5359 (2006).
31. Yelamos, J. *et al.* PARP-2 deficiency affects the survival of $CD4^+CD8^+$ double-positive thymocytes. *EMBO J.* **25**, 4350–4360 (2006).
32. Kofler, J. *et al.* Differential effect of PARP-2 deletion on brain injury after focal and global cerebral ischemia. *J. Cereb. Blood Flow Metab.* **26**, 135–141 (2006).
33. Ma, Q., Baldwin, K.T., Renzelli, A.J., McDaniel, A. & Dong, L. TCDD-inducible poly(ADP-ribose) polymerase: a novel response to 2,3,7,8-tetrachlorodibenzo-p-dioxin. *Biochem. Biophys. Res. Commun.* **289**, 499–506 (2001).
34. Kutsch, S., Degrandi, D. & Pfeffer, K. Immediate lymphotoxin β receptor-mediated transcriptional response in host defense against L. monocytogenes. *Immunobiology* **213**, 353–366 (2008).
35. Kato, H. *et al.* Length-dependent recognition of double-stranded ribonucleic acids by retinoic acid-inducible gene-I and melanoma differentiation-associated gene 5. *J. Exp. Med.* **205**, 1601–1610 (2008).
36. Chiu, Y.H., Macmillan, J.B. & Chen, Z.J. RNA polymerase III detects cytosolic DNA and induces type I interferons through the RIG-I pathway. *Cell* **138**, 576–591 (2009).
37. Ablasser, A. *et al.* RIG-I-dependent sensing of poly(dA:dT) through the induction of an RNA polymerase III-transcribed RNA intermediate. *Nat. Immunol.* **10**, 1065–1072 (2009).
38. Kerns, J.A., Emerman, M. & Malik, H.S. Positive selection and increased antiviral activity associated with the PARP-containing isoform of human zinc-finger antiviral protein. *PLoS Genet.* **4**, e21 (2008).
39. Guo, X., Carroll, J.W., Macdonald, M.R., Goff, S.P. & Gao, G. The zinc finger antiviral protein directly binds to specific viral mRNAs through the CCCH zinc finger motifs. *J. Virol.* **78**, 12781–12787 (2004).
40. Wang, N. *et al.* Viral induction of the zinc finger antiviral protein is IRF3-dependent but NF-κB-independent. *J. Biol. Chem.* **285**, 6080–6090 (2010).
41. Bowzard, J.B., Ranjan, P., Sambhara, S. & Fujita, T. Antiviral defense: RIG-Ing the immune system to STING. *Cytokine Growth Factor Rev.* **20**, 1–5 (2009).
42. Saito, T. *et al.* Regulation of innate antiviral defenses through a shared repressor domain in RIG-I and LGP2. *Proc. Natl. Acad. Sci. USA* **104**, 582–587 (2007).
43. Cui, S. *et al.* The C-terminal regulatory domain is the RNA 5′-triphosphate sensor of RIG-I. *Mol. Cell* **29**, 169–179 (2008).
44. Schmidt, A. *et al.* 5′-triphosphate RNA requires base-paired structures to activate antiviral signaling via RIG-I. *Proc. Natl. Acad. Sci. USA* **106**, 12067–12072 (2009).
45. Kato, H. *et al.* Differential roles of MDA5 and RIG-I helicases in the recognition of RNA viruses. *Nature* **441**, 101–105 (2006).
46. Urnov, F. *et al.* Highly efficient endogenous human gene correction using designed zinc-finger nucleases. *Nature* **435**, 646–651 (2005).
47. Foley, J. *et al.* Targeted mutagenesis in zebrafish using customized zinc-finger nucleases. *Nat. Protocols* **4**, 1855–1867 (2009).
48. Lee, H., Kim, E. & Kim, J. Targeted chromosomal deletions in human cells using zinc finger nucleases. *Genome Res.* **20**, 81–89 (2010).
49. Yuan, W. & Krug, R. Influenza B virus NS1 protein inhibits conjugation of the interferon (IFN)-induced ubiquitin-like ISG15 protein. *EMBO J.* **20**, 362–371 (2001).
50. Arimoto, K. *et al.* Negative regulation of the RIG-I signaling by the ubiquitin ligase RNF125. *Proc. Natl. Acad. Sci. USA* **104**, 7500–7505 (2007).
51. Friedman, C. *et al.* The tumour suppressor CYLD is a negative regulator of RIG-I-mediated antiviral response. *EMBO Rep.* **9**, 930–936 (2008).
52. Oshiumi, H., Matsumoto, M., Hatakeyama, S. & Seya, T. Riplet/RNF135, a RING finger protein, ubiquitinates RIG-I to promote interferon-beta induction during the early phase of viral infection. *J. Biol. Chem.* **284**, 807–817 (2009).
53. Saito, T., Owen, D.M., Jiang, F., Marcotrigiano, J. & Gale, M. Jr. Innate immunity induced by composition-dependent RIG-I recognition of hepatitis C virus RNA. *Nature* **454**, 523–527 (2008).

Bone Marrow Transplantation (2010) 45, 1594–1601

www.nature.com/bmt

ORIGINAL ARTICLE

Identification of molecular markers for pre-engraftment immune reactions after cord blood transplantation by SELDI-TOF MS

Y Morita-Hoshi[1], S-I Mori[1], A Soeda[1], T Wakeda[1], Y Ohsaki[2], M Shiwa[2], K Masuoka[3], A Wake[3], S Taniguchi[3], Y Takaue[1] and Y Heike[1]

[1]*Department of Medical Oncology, National Cancer Center Hospital, Tokyo, Japan;* [2]*Bio-Rad Laboratories, K.K., Kanagawa, Japan and* [3]*Department of Hematology, Toranomon Hospital, Tokyo, Japan*

Cord blood transplantation (CBT) is frequently associated with pre-engraftment immune reaction (PIR), which is characterized by high-grade fever that peaks around day 9 of transplantation. PIR mimics hyperacute GVHD or engraftment syndrome; however, it is considered to be of different etiology as it occurs before engraftment. Proteomic patterns have been studied in the fields of transplantation, but no specific marker has been identified. As there are no data to confirm the mechanism of PIR, we used a surface-enhanced laser desorption/ionization time-of-flight mass spectroscopy (SELDI-TOF MS) system to identify a specific marker for PIR. The protein expression profile of serum samples from CBT patients was analyzed with a SELDI-TOF MS system. A protein peak that commonly predominated in PIR was purified by an anion exchange column, isolated by SDS-PAGE, and identified by in-gel trypsin digestion, and mass fingerprinting. A 8.6-kDa protein and 11-kDa protein that increased by 10- to 100-fold in the serum of patients during PIR was identified as anaphylatoxin C4a and serum amyloid A. SELDI-TOF MS system in combination with other proteomic methods could serve as a potential diagnostic tool in discovering biomarkers for PIR after CBT.

Bone Marrow Transplantation (2010) **45,** 1594–1601; doi:10.1038/bmt.2010.18; published online 15 March 2010
Keywords: serum amyloid A; pre-engraftment immune reactions; cord blood transplantation; SELDI-TOF MS

Introduction

High-grade fever before engraftment without any other obvious signs of infection, which mimics hyperacute GVHD or engraftment syndrome, is frequently observed in patients who undergo cord blood transplantation (CBT).[1,2] In previous reports, when patients with no evidence of infection or adverse effects of medication exhibited skin eruption, diarrhea, jaundice or body weight gain greater than 10% of baseline, these conditions were defined as 'immune reactions.' These reactions were classified as 'pre-engraftment immune reaction (PIR)' if they developed 6 or more days before engraftment, whereas those within 5 days of engraftment were defined as 'engraftment syndrome' (1). The reported incidence of PIR has ranged from 78–83% (1–2). This PIR peaks at around day 9 of CBT, and is often accompanied by high-grade fever. Although PIR responds well to corticosteroid therapy, the prolonged use of steroid often causes an increased incidence of infectious complications, leading to significant treatment-related mortality, particularly in the elderly. GVHD prophylaxis with tacrolimus, compared with CsA, is less likely to be associated with PIR[3,4] and the addition of MTX may further reduce the risk.[5,6] It has been speculated that cytokines induced by the initial immune/inflammation reaction are the primary cause of PIR, but no data are available to confirm this supposition. To clarify this question, we evaluated the protein expression profile of serum in CBT recipients using a surface-enhanced laser desorption/ionization time-of-flight mass spectroscopy (SELDI-TOF MS) system and found potential markers for PIR.

Materials and methods

Study patients and samples

Patients who received treatment for hematological malignancies at the National Cancer Center Hospital or Toranomon Hospital between February 2002 and May 2005 were included in this study. The study was approved by the Ethics Committee, and written informed consent was given by all patients. A total of 78 peripheral blood samples taken from 57 patients, including 34 samples taken from 13 patients who had undergone allogeneic CBT, were eligible for the analysis. Samples from CBT patients were taken on three different occasions, that is, (1) afebrile period before PIR onset: the median of day 3 (1–6) post transplant; (2) onset of fever: the median of day 8 (6–13); and (3) after resolution of fever: the median of day 26.5 (15–60). To analyze the protein profile that was specific to PIR, samples taken from patients with documented infection

Correspondence: Dr Y Heike, Department of Medical Oncology, National Cancer Center Hospital, 5-1-1 Tsukiji Chuo-ku, Tokyo 104-0045, Japan.
E-mail: yheike@ncc.go.jp
Received 14 July 2009; revised 24 December 2009; accepted 27 December 2009; published online 15 March 2010

Table 1 Characteristics of 13 patients

Age	
Median 52 years	
Range (26–70 years)	
Sex	
Male	6
Female	7
Primary disease	
AML	5
ALL	2
Adult T-cell leukemia	2
Diffuse large B-cell lymphoma	2
Peripheral T-cell lymphoma-unspecified	1
Myelofibrosis	1
Conditioning regimen	
Flu 180 mg/m^2, BU 8 mg/kg, TBI 4 Gy	6
Flu 180 mg/m^2, BU 8 mg/kg, TBI 8 Gy	1
Flu 125 mg/m^2, Mel 80 mg/m^2, TBI 4 Gy	5
Flu 125 mg/m^2, Mel 80 mg/m^2, TBI 2 Gy	1
GVHD Prophylaxis	
CsA	6
CsA + short-term MTX	4
Tacrolimus	3
No. of HLA mismatch	
1 locus	3
2 loci	9
4 loci	1
Day of engraftment (n = 11)	
Median 18 days	
Range 13–29 days	
Day of PIR onset	
Median 8 days	
Range 6–13 days	
Day between PIR and resolution	
Median 15.5 days	
Range 7–49 days	
Treatment for PIR	
None	3
Empiric antibiotics	4
Corticosteroids and empiric antibiotics	6

Abbreviations: Flu = fludarabine; Mel = melphalan; PIR = pre-engraftment immune reaction.

or those who were suffering from engraftment syndrome were excluded from the analysis. All 13 CBT patients received reduced-intensity conditioning, and graft rejection occurred in 2 patients (16%). As for the treatment and its outcome for PIR, six patients responded well to corticosteroid and seven patients improved without any treatment or empiric antibiotics alone. One of the patients who developed graft failure received corticosteroids for the treatment of PIR. The mean neutrophil count at PIR was 15 (0–100)/μl. The patients' characteristics are shown in Table 1.

SELDI-TOF MS analysis

The relative protein expression levels were determined as previously described with the following modifications using a SELDI TOF-MS system (Bio-Rad Laboratories, Hercules, CA, USA).[7,8] The protein was processed using a Biomek 2000 Laboratory Work Station (Beckman Coulter, Fullerton, CA, USA). Samples were analyzed in duplicate and 28 spectra were obtained from five serum fractions with four kinds of chips (IMAC30, CM10, H50, Q10), four different binding buffers, two kinds of energy absorption molecules and two focus mass ranges.

Serum fractionation

The serum samples were centrifuged at 20 000 × *g* and the supernatant was vigorously mixed with denaturation buffer U9 (9 M urea: 2% CHAPS: 50 mM Tris-HCl, pH9) for 20 min. Serum samples were fractionated into four fractions by the following methods. Briefly, the strong anion exchange resin BioSepra Q Ceramic HyperD F (Pall, NY, USA) was equilibrated with 50 mM Tris-HCl, pH 9, in advance, and 180 μl per well was loaded onto a filter plate. The loaded resin was equilibrated three times with 200 μl of U1 buffer (U9 buffer diluted 1:10 with 50 mM Tris-HCl). Denatured serum was added to the resin, the sample well was washed with 50 μl of U1 buffer, and the sample was incubated for 30 min at 4 °C. The non-binding fraction was collected, and protein was eluted by a phased pH gradient at pH 5.8, pH 4 and below pH 4.

Protein binding

IMAC30 (immobilized metal affinity capture), CM10 (cation exchange), H50 (reverse-phase) and Q10 (anion exchange) ProteinChip arrays were used for the analysis. To immobilize copper ion on the IMAC30 surface, each spot was incubated with 50 μl of 100 mM copper sulfate for 10 min at room temperature. Excess copper was removed by washing twice with distilled water and incubated with 50 μl of 100 mM sodium acetate (pH 4) for 5 min at room temperature. Each spot was rinsed twice with distilled water before the analysis step.

The following buffers were used for binding and dilution of the samples: 100 mM sodium acetate (pH 4) or 50 mM HEPES (pH 7) for CM10, 100 mM sodium phosphate (pH 7) + 0.5 M NaCl for IMAC30, 50 mM HEPES (pH 7) for H50, and 50 mM Tris-HCl (pH 8) for Q10. The following procedure was commonly used for all chip analyses: (1) Each spot was equilibrated twice with 150 μl of binding buffer on a shaker for 5 min, and excess buffer was removed. (2) The fractionated and unfractionated samples were diluted 10-fold with binding buffer. The diluted samples were loaded onto a chip, and incubated on a shaker for 30 min at room temperature. (3) The chip was washed three times on a shaker for 5 min with 150 μl per spot of buffer. (4) The chip was rinsed twice with 200 μl of distilled water and dried. (5) Each spot was treated with two kinds of energy absorption molecules: 50% saturated sinapinic acid and α-cyano-4-hydroxycinnamic acid.

Protein detection

Captured proteins were detected using a ProteinChip SELDI system (PCS4000 Enterprise, Bio-Rad Laboratories). The maximum detection range was 100 000 with a focus mass range of 3000–10 000 for low MW, and 200 000 with a focus mass range of 10 000–30 000 for high MW. Quantitative analysis of proteins was performed using

ProteinChip Software version 3.2 and ProteinChip Data Manager Software (Bio-Rad Laboratories).

Protein purification and identification

The serum samples were denatured with urea and fractionated by an anion exchange column (ProteinChip Q Spin Columns, Bio-Rad Laboratories) to remove albumin by binding it to the column. The fraction that passed through the anion exchange column at pH 9 was collected. The sample was diluted threefold with 50 mM Tris-HCl (pH 8) and loaded onto an anion exchange column to bind the objective peak protein. The protein was eluted in a phased manner with 50–300 mM NaCl. After demineralization and concentration, the proteins were separated by SDS-PAGE and stained with Coomassie Brilliant Blue. In-gel digestion by Trypsin was performed on the objective band. The protein was determined by mass fingerprinting of the digested peaks against the ProFound database (Rockefeller University

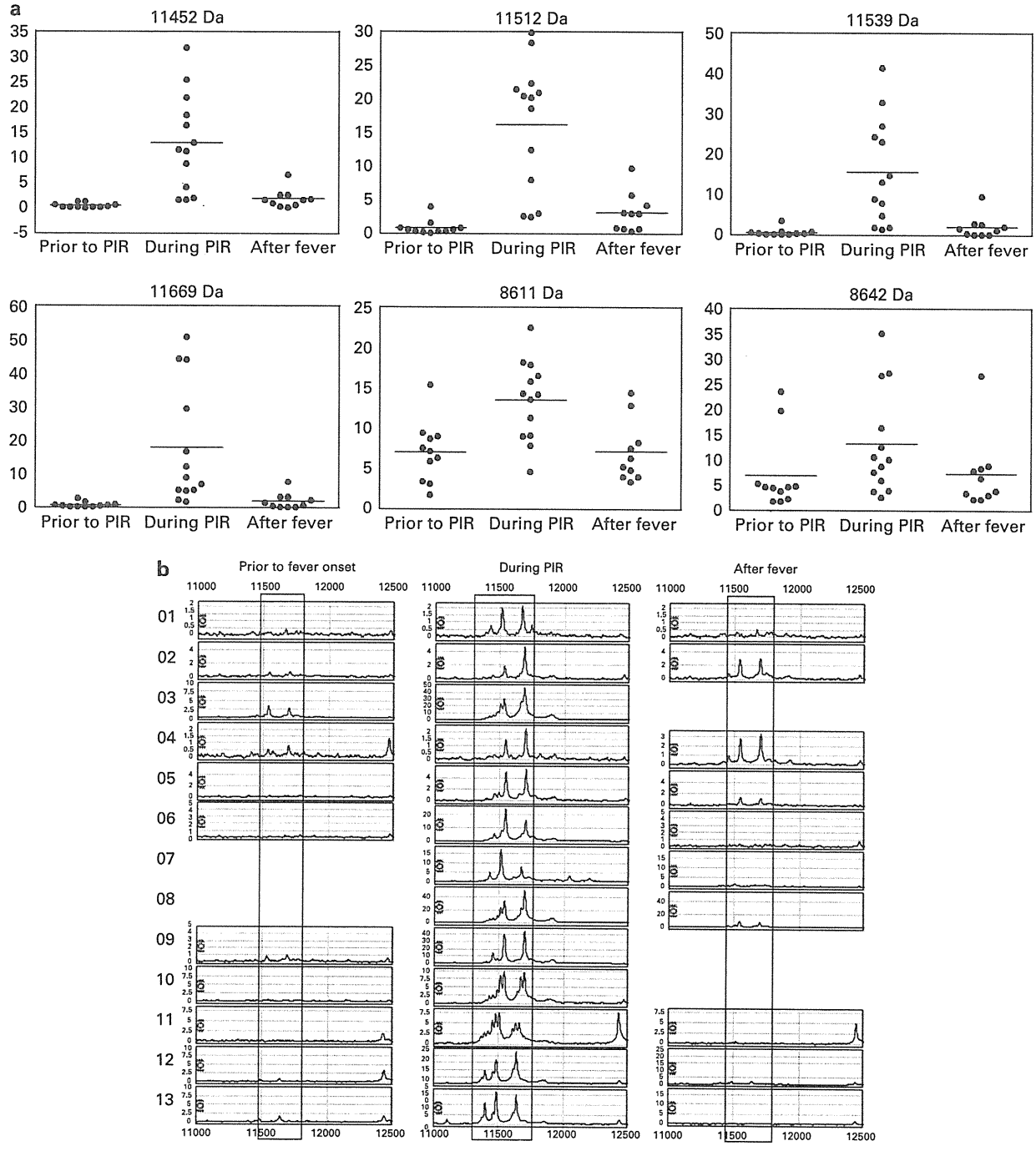

Figure 1 (**a**) Peak intensity levels of six protein peaks that commonly increased at the time of PIR. (**b**) Typical response pattern of the 11-kDa protein peak in 13 patients, in a trace view.

edition), and the amino-acid sequence was determined using the PCI-QSTAR MS/MS search engine.

Statistical analysis

Data were analyzed using ProteinChip Data Manager Software. After baseline correction, MW calibration was performed using eight standard protein molecules followed by a total ion current normalization process. To identify distinct and significant peaks, we used a signal-to-noise cutoff of 2 ($s/n > 2$), which selects peaks with a signal level that is significantly above the calculated background noise.

For the statistical analysis, the Kruskal–Wallis H-test was used to compare differences among three groups. The differences between the two groups were compared with the Wilcoxon–Mann–Whitney *U*-test. Probabilities of $P < 0.05$ were defined as statistically significant.

Results

Protein profiles

A total of 3005 protein peaks for which $s/n > 2$ were detected. Of these, 743 showed a significant difference between the febrile and afebrile periods. After we further excluded noise peaks, 469 peaks still showed a significant difference, and after excluding variations between individuals, 19 candidate peaks that were commonly elevated at PIR in more than 11 patients (84.6%) were selected. Reproducibility was tested, and six protein peaks that commonly increased at the time of PIR, with molecular masses of 8611, 8642, 11452, 11512, 11539 and 11669 Da, were identified (Figure 1). The assay conditions under which the proteins were identified are shown in Table 2.

Purification and determination of target proteins

Protein peaks were fractionated by an anion exchange column, and the elution fraction at pH 9 was used for purification and identification because the albumin that overlaps the candidate peak was removed from this fraction. The protein was eluted from the column with 100–150 mM NaCl. SDS-PAGE after demineralization and concentration of the protein showed an 11-kDa band (Figure 2a). In-gel digestion was performed on the cutout band, and mass fingerprinting was performed for eight peptides with mass values of 1455, 1463, 1550, 1611, 1670, 1706, 1941 and 2097 (Figure 2b). Six of these values were consistent with serum amyloid A (SAA), which consists of

Table 2 Assay conditions by which marker proteins were detected

MW	*Fraction*	*Chip*	*Binding buffer*	*EAM*	*Focus mass range*
8611	pH 9	CM10	100 mM Na Acetate (pH 4)	SPA	3000–10 000
8642	pH 9	CM10	50 mM HEPES (pH 7)	SPA	3000–10 000
11452	Unfractionated	IMAC30	100 mM Na Phosphate (pH 7) +0.5 M NaCl	SPA	10 000–30 000
11512	Unfractionated	IMAC30	100 mM Na Phosphate (pH 7) +0.5 M NaCl	SPA	10 000–30 000
	pH 9	CM10	50 mM HEPES (pH 7)	SPA	10 000–30 000
11539	Unfractionated	Q10	50 mM Tris-HCl (pH 8)	SPA	10 000–30 000
11669	Unfractionated	IMAC30	100 mM Na Phosphate (pH 7) +0.5 M NaCl	SPA	10 000–30 000
	pH 9	CM10	50 mM HEPES (pH 7)	SPA	10 000–30 000
	Unfractionated	Q10	50 mM Tris-HCl (pH 8)	SPA	10 000–30 000

Abbreviations: CM10 = cation exchange; EAM = energy absorption molecule; IMAC30 = immobilized metal affinity capture; SPA = 50% saturated sinapinic acid; Q10 = anion exchange.

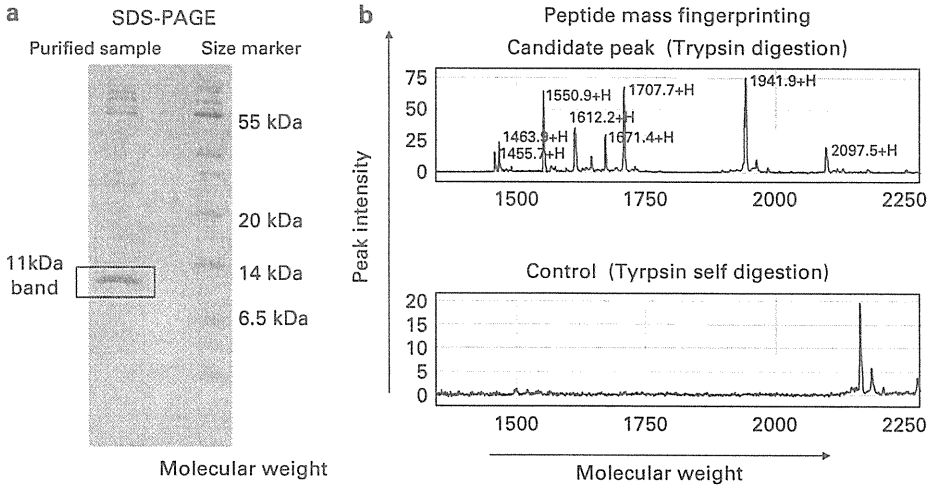

Figure 2 Representative data of SDS-PAGE and peptide mass fingerprinting from the sample taken during PIR. (a) SDS-PAGE showing the 11-kDa band. Coomassie Brilliant Blue (CBB) staining. (b) Peptide mass fingerprinting of the marker protein.

104 amino acids and has a MW of 11 622, or its isoforms, in which serine and/or arginine is deleted from the N-terminal portion (Figure 3). The amino-acid sequences of all six peptide masses were consistent with SAA by MS/MS analysis.

The SAA level was measured by ELISA in the same sample that was assessed by SELDI-TOF MS. The mean SAA level measured by ELISA before fever onset was 14 (3–51) μg/ml, and this increased to 883 (40–2470) μg/ml at the time of PIR and decreased to 45 (8–126) μg/ml after resolution of the fever (Figure 4a). The data obtained by ELISA agreed with the SELDI-TOF MS peak intensity value (Figure 4b). Although the 8.6 kDa peak was not determined in this experiment, it was most likely to be anaphylatoxin C4a based on its MW (8650) and isoelectric point (9.45).

Serum amyloid A value in different conditions

Seven of the 13 patients with PIR developed acute GVHD, and 2 patients had graft failure. The patients who developed graft failure showed high levels of SAA at PIR (2040 and 2390 μg/ml). The mean and median values of SAA at PIR in seven patients who developed acute GVHD were 677 μg/ml and 451 (60–2470) μg/ml, respectively, which were not significantly different from the values in the four patients without acute GVHD (432 and 506 (40–675) μg/ml) ($P = 0.93$).

The SAA value was assessed in 24 non-transplant febrile patients: (a) 12 samples from patients with documented infection, including sepsis, (b) 6 samples from patients with tumor fever and (c) 6 samples from patients with drug-induced fever. The mean and median values and statistical significance when compared with PIR were (a) 477 μg/ml and 347 (31–1240) μg/ml ($P = 0.63$), (b) 432 μg/ml and 248 (127–1080) μg/ml ($P = 0.75$) and (c) 49 μg/ml and 42 (31–73) μg/ml ($P = 0.0013$), respectively.

The SAA values during acute GVHD in other transplantation settings were assessed in 20 patients: (d) 10 samples from related allo-PBSCT recipients including 5 febrile patients and (e) 10 samples from unrelated BMT recipients including 4 febrile patients. The mean and median values and statistical significance when compared with PIR were (d) 293 and 238 (19–645) μg/ml ($P = 0.20$) and (e) 366 and 344 (31–724) μg/ml ($P = 0.31$), respectively (Figure 4a). The level of SAA elevation was not as high as that in PIR, but the sample size was too small to show specificity.

Discussion

Proteomic analysis has been widely used to assess the allogeneic response, including GVHD in hematopoietic SCT.[8–11] The two most important methods that are used to investigate biomarkers, for example, detection of early GVHD, are SELDI-TOF MS and capillary zone electrophoresis mass spectrometry (CE-MS). Although the resolution and sensitivity of SELDI-TOF MS are not as high as those of CE-MS, it has the benefits of relatively low cost and ease of use.[9] It has been reported that proteomic pattern analysis by SELDI-TOF MS can be used to accurately distinguish GVHD samples from post transplant non-GVHD samples and pretransplant samples with 100% specificity and 100% sensitivity.[8] Furthermore, with the CE-MS system, 16 polypeptide patterns excreted in the urine could be used to discriminate patients with GVHD from patients without complications, with 82% specificity and 100% sensitivity. In addition, 13 sepsis-specific polypeptides

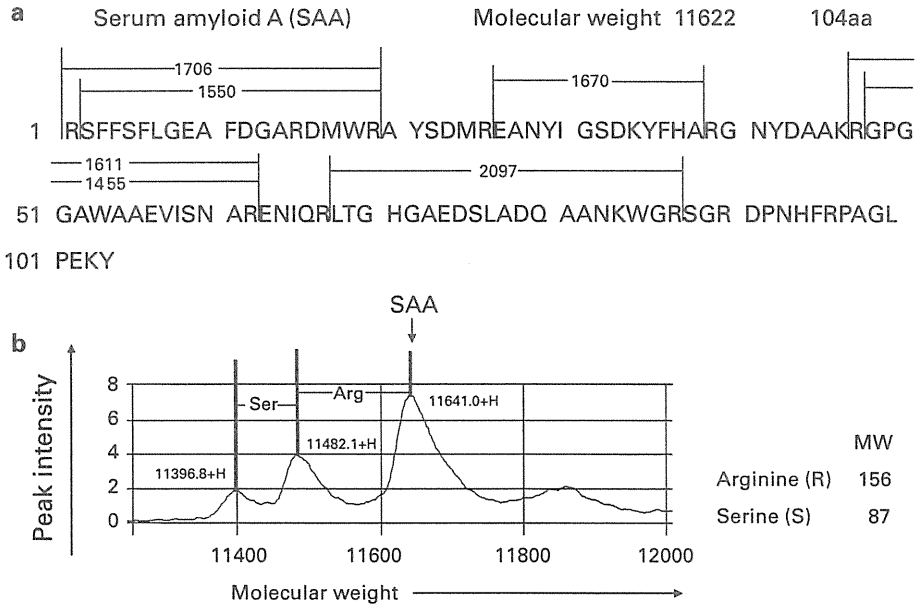

Figure 3 (a) Amino-acid sequences of the target protein. Six peptide sequences that matched an MS/MS database search were identical to amino acids of SAA. (b) The analyzed peak was determined to be SAA and its isoform produced by the deletion of serine and/or arginine from the N terminus.

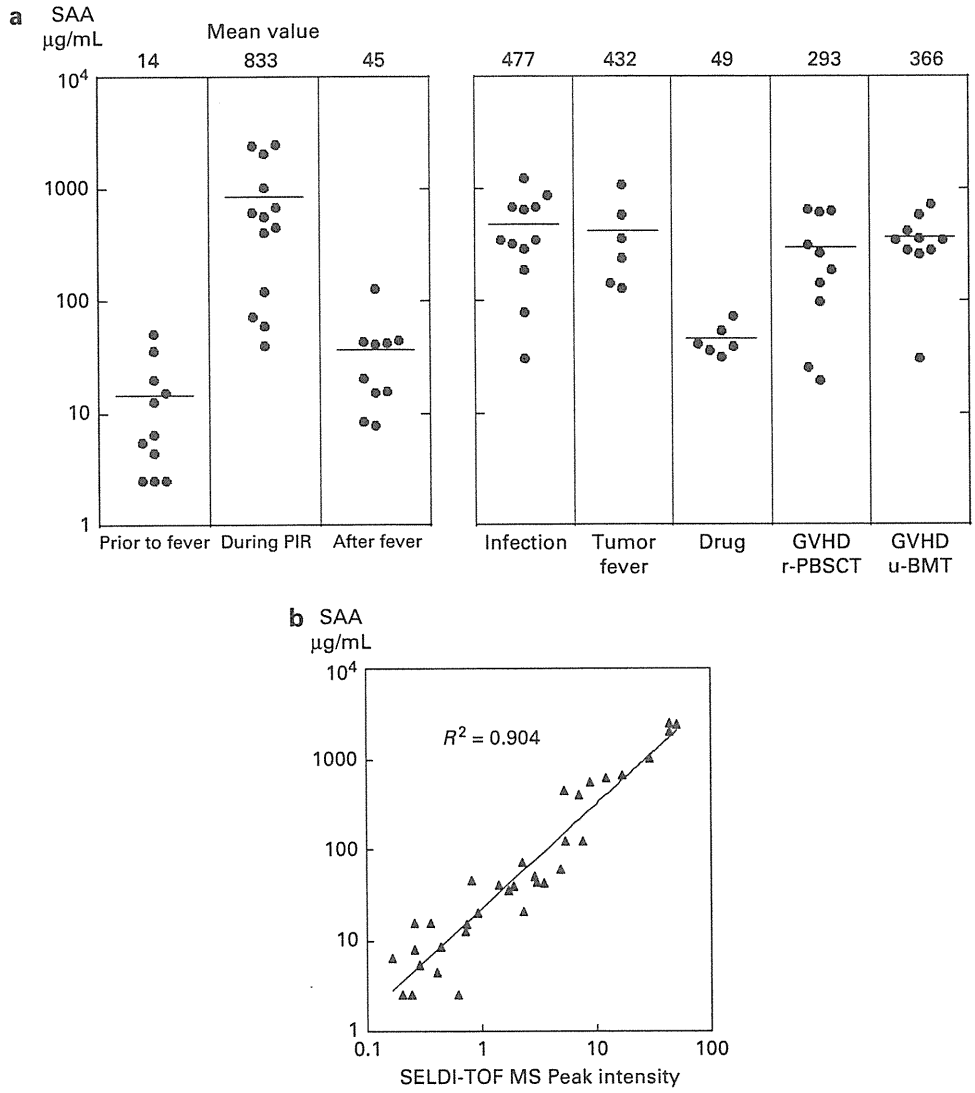

Figure 4 SAA level measured by ELISA. (**a**) SAA level in different conditions: Before fever, during PIR and after fever resolution in 13 CBT recipients. Documented infection including sepsis, tumor fever, drug-induced fever, GVHD in related allo-PBSCT (r-PBSCT) and GVHD in unrelated BMT (u-BMT). (**b**) The data obtained by ELISA correlated well with the SELDI-TOF MS peak intensity value ($n = 34$).

could be used to distinguish sepsis from GVHD, with a specificity of 97% and a sensitivity of 100%.[10] The diagnosis of acute GVHD, even before a clinical diagnosis, is possible with the use of a GVHD-specific model consisting of 31 polypeptides.[11]

Proteomic analysis has also been applied to the analysis of an allograft response in organ transplantation in animal models.[12,13] In a mouse skin transplant model, several protein biomarker candidates were detected by ProteinChip technology based on their molecular mass, which could be used to clearly differentiate between rejection and non-rejection groups, before a clinical manifestation.[12] In a rat small bowel transplantation model, two migration inhibitory factor-related proteins and lysozyme that increased during allograft rejection were identified by a SELDI-TOF MS system.[13] Thus, we believe that ProteinChip technology should be a useful tool for identifying specific markers related to PIR.

Previous studies have shown that combinations of several biomarkers are more sensitive and accurate than the use of a single marker in the diagnosis of an allogeneic response.[11] However, most biomarkers are not well characterized and can only be detected by the ProteinChip system. As the ProteinChip system is not routinely available in clinical practice, we thought it would be necessary to identify a marker that could be monitored easily. In this study, SAA was identified as a candidate marker for PIR. Furthermore, this study showed the feasibility of quantitative analysis by the ProteinChip system, although the ProteinChip system has previously been considered to be a tool for semiquantitative analysis.

Serum biomarkers associated with leukemia[14] and cancer[15–21] have also been identified by the SELDI

ProteinChip technique. In some of these studies, SAA has been reported to be a potential marker for particular cancer status. Multiple variants of SAA have been detected by the SELDI ProteinChip technique in renal cancer patients.[20] The SELDI ProteinChip technique revealed that SAA may be a biomarker for identifying prostate cancer patients with bone lesions, with a sensitivity and specificity of 89.5%.[21]

SAA activates human mast cells, which leads to the degradation of SAA and the generation of an amyloidogenic SAA fragment.[22] SAA is a major acute-phase reactant that increases by as much as 1000-fold during inflammation. SAA is potentially involved in the pathogenesis of several chronic inflammatory diseases: it is the precursor of amyloid A protein deposited in amyloid A amyloidosis, and has also been implicated in the pathogenesis of atherosclerosis and rheumatoid arthritis.[23,24] SAA may be closely related to poor patient outcomes, including left ventricular systolic dysfunction, cardiac rupture and mortality in acute myocardial infarction.[25,26]

Some studies have suggested that the elevation of SAA may be associated with acute allograft rejection of the kidney,[27–30] liver[31] and heart.[32] By contrast, it has also been reported that SAA is inadequate for predicting acute rejection in cardiac allograft.[33] With regard to renal allograft rejection, SAA was shown to be a sensitive marker that rose above 100 mg/l in all cases of rejection, whereas C-reactive protein (CRP) showed little or no response to rejection.[29] We could not confirm whether or not the elevation of SAA was a phenomenon that occurs with all CBT around day 9, as the value of SAA in samples from non-febrile patients at this time point was not analyzed. However, it is unlikely that the elevation of SAA occurs with all allogeneic transplantation, as the phenomenon was not prominent in patients with acute GVHD. The possibility that the elevation of SAA was only a consequence of acute phase change that occurs with high-grade fever could not be completely ruled out, as the elevation of SAA was not confined to CBT; however, the elevation level was higher in PIR than in other conditions. Furthermore, patients who developed graft rejection had markedly higher levels of SAA. Although the reason for these observations is unclear, a previous report on SAA as an indication of allograft rejection has suggested that inflammation and cytokine production induced by an allo-reaction may be related to the elevation of SAA in PIR.

In the case of CBT, SAA that increases in relation to PIR, as a factor associated with a poor prognosis of CBT, may be related to allograft rejection. Our retrospective study showed that pre-engraftment CRP values may predict acute GVHD and nonrelapse mortality.[34] Although CRP elevation was also observed during PIR, SAA elevation was more rapid and prominent. The SAA level was above the normal limit in all 13 samples at the day of fever onset, whereas 2 samples were within the normal limit for CRP. The mean SAA level was 121 times the upper normal limit at day 2 of fever onset, whereas the mean CRP level was 10 times the upper normal limit at the same time. SAA or anaphylatoxin C4a alone may lack specificity as a marker for PIR. However, the further analysis of samples obtained from CBT recipients by our method may provide fingerprints of markers useful for the diagnosis of PIR. Identification of peak markers suggests that the SELDI-TOF MS system in combination with other proteomic methods could serve as a potential diagnostic tool in discovering biomarkers for PIR after CBT.

Conflict of interest

The authors declare no conflict of interest.

Acknowledgements

This work was supported in part by grants from the Ministry of Health, Labor and Welfare, Japan.

References

1 Kishi Y, Kami M, Miyakoshi S, Kanda Y, Murashige N, Teshima T *et al.* Early immune reaction after reduced-intensity cord-blood transplantation for adult patients. *Transplantation* 2005; **80**: 34–40.
2 Miyakoshi S, Yuji K, Kami M, Kusumi E, Kishi Y, Kobayashi K *et al.* Successful engraftment after reduced-intensity umbilical cord blood transplantation for adult patients with advanced hematological diseases. *Clin Cancer Res* 2004; **10**: 3586–3592.
3 Uchida N, Wake A, Takagi S, Yamamoto H, Kato D, Matsuhashi Y *et al.* Umbilical cord blood transplantation after reduced-intensity conditioning for elderly patients with hematologic diseases. *Biol Blood Marrow Transplant* 2008; **14**: 583–590.
4 Takahashi S, Iseki T, Ooi J, Tomonari A, Takasugi K, Shimohakamada Y *et al.* Single-institute comparative analysis of unrelated bone marrow transplantation and cord blood transplantation for adult patients with hematologic malignancies. *Blood* 2004; **104**: 3813–3820.
5 Narimatsu H, Terakura S, Matsuo K, Oba T, Uchida T, Iida H *et al.* Short-term methotrexate could reduce early immune reactions and improve outcomes in umbilical cord blood transplantation for adults. *Bone Marrow Transplant* 2007; **39**: 31–39.
6 Mori T, Aisa Y, Nakazato T, Yamazaki R, Shimizu T, Mihara A *et al.* Tacrolimus and methotrexate for the prophylaxis of graft-versus-host disease after unrelated donor cord blood transplantation for adult patients with hematologic malignancies. *Transplant Proc* 2007; **39**: 1615–1619.
7 Heike Y, Hosokawa M, Osumi S, Fujii D, Aogi K, Takigawa N *et al.* Identification of serum proteins related to adverse effects induced by docetaxel infusion from protein expression profiles of serum using SELDI ProteinChip system. *Anticancer Res* 2005; **25**: 1197–1203.
8 Srinivasan R, Daniels J, Fusaro V, Lundqvist A, Killian JK, Geho D *et al.* Accurate diagnosis of acute graft-versus-host disease using serum proteomic pattern analysis. *Exp Hematol* 2006; **34**: 796–801.
9 Weissinger EM, Mischak H, Ganser A, Hertenstein B. Value of proteomics applied to the follow-up in stem cell transplantation. *Ann Hematol* 2006; **85**: 205–211.
10 Kaiser T, Kamal H, Rank A, Kolb HJ, Holler E, Ganser A *et al.* Proteomics applied to the clinical follow-up of patients after allogeneic hematopoietic stem cell transplantation. *Blood* 2004; **104**: 340–349.

11 Weissinger EM, Schiffer E, Hertenstein B, Ferrara JL, Holler E, Stadler M *et al.* Proteomic patterns predict acute graft-versus-host disease after allogeneic hematopoietic stem cell transplantation. *Blood* 2007; **109**: 5511–5519.
12 El Essawy B, Otu HH, Choy B, Zheng XX, Libermann TA, Strom TB. Proteomic analysis of the allograft response. *Transplantation* 2006; **82**: 267–274.
13 Yamayoshi Y, Watanabe T, Tanabe M, Hoshino K, Matsumoto K, Morikawa Y *et al.* Novel application of ProteinChip technology exploring acute rejection markers of rat small bowel transplantation. *Transplantation* 2006; **82**: 320–326.
14 Albitar M, Potts SJ, Giles FJ, O'Brien S, Keating M, Thomas D *et al.* Proteomic-based prediction of clinical behavior in adult acute lymphoblastic leukemia. *Cancer* 2006; **106**: 1587–1594.
15 Koopmann J, Zhang Z, White N, Rosenzweig J, Fedarko N, Jagannath S *et al.* Serum diagnosis of pancreatic adenocarcinoma using surface-enhanced laser desorption and ionization mass spectrometry. *Clin Cancer Res* 2004; **10**: 860–868.
16 Wong YF, Cheung TH, Lo KW, Wang VW, Chan CS, Ng TB *et al.* Protein profiling of cervical cancer by protein-biochips: proteomic scoring to discriminate cervical cancer from normal cervix. *Cancer Lett* 2004; **211**: 227–234.
17 Yang SY, Xiao XY, Zhang WG, Zhang LJ, Zhang W, Zhou B *et al.* Application of serum SELDI proteomic patterns in diagnosis of lung cancer. *BMC Cancer* 2005; **5**: 83.
18 Ward DG, Suggett N, Cheng Y, Wei W, Johnson H, Billingham LJ *et al.* Identification of serum biomarkers for colon cancer by proteomic analysis. *Br J Cancer* 2006; **94**: 1898–1905.
19 Malik G, Ward MD, Gupta SK, Trosset MW, Grizzle WE, Adam BL *et al.* Serum levels of an isoform of apolipoprotein A-II as a potential marker for prostate cancer. *Clin Cancer Res* 2005; **11**: 1073–1085.
20 Tolson J, Bogumil R, Brunst E, Beck H, Elsner R, Humeny A *et al.* Serum protein profiling by SELDI mass spectrometry: detection of multiple variants of serum amyloid alpha in renal cancer patients. *Lab Invest* 2004; **84**: 845–856.
21 Le L, Chi K, Tyldesley S, Flibotte S, Diamond DL, Kuzyk MA *et al.* Identification of serum amyloid A as a biomarker to distinguish prostate cancer patients with bone lesions. *Clin Chem* 2005; **51**: 695–707.
22 Niemi K, Baumann MH, Kovanen PT, Eklund KK. Serum amyloid A (SAA) activates human mast cells which leads into degradation of SAA and generation of an amyloidogenic SAA fragment. *Biochim Biophys Acta* 2006; **1762**: 424–430.
23 Uhlar CM, Whitehead AS. Serum amyloid A, the major vertebrate acute-phase reactant. *Eur J Biochem* 1999; **265**: 501–523.
24 Salazar A, Pinto X, Mana J. Serum amyloid A and high-density lipoprotein cholesterol: serum markers of inflammation in sarcoidosis and other systemic disorders. *Eur J Clin Invest* 2001; **31**: 1070–1077.
25 Katayama T, Nakashima H, Takagi C, Honda Y, Suzuki S, Iwasaki Y *et al.* Serum amyloid a protein as a predictor of cardiac rupture in acute myocardial infarction patients following primary coronary angioplasty. *Circ J* 2006; **70**: 530–535.
26 Katayama T, Nakashima H, Honda Y, Suzuki S, Yamamoto T, Iwasaki Y *et al.* The relationship between acute phase serum amyloid A (SAA) protein concentrations and left ventricular systolic function in acute myocardial infarction patients treated with primary coronary angioplasty. *Int Heart J* 2007; **48**: 45–55.
27 Muller TF, Trosch F, Ebel H, Grussner RW, Feiber H, Goke B *et al.* Pancreas-specific protein (PASP), serum amyloid A (SAA), and neopterin (NEOP) in the diagnosis of rejection after simultaneous pancreas and kidney transplantation. *Transpl Int* 1997; **10**: 185–191.
28 Maury CP, Teppo AM, Ahonen J, von Willebrand E. Measurement of serum amyloid A protein concentrations as test of renal allograft rejection in patients with initially non-functioning grafts. *Br Med J (Clin Res Ed)* 1984; **288**: 360–361.
29 Hartmann A, Eide TC, Fauchald P, Bentdal O, Herbert J, Gallimore JR *et al.* Serum amyloid A protein is a clinically useful indicator of acute renal allograft rejection. *Nephrol Dial Transplant* 1997; **12**: 161–166.
30 Fukuda Y, Hoshino S, Tanaka I, Yoneya T, Takeshita T, Sumimoto R *et al.* Examination of serum amyloid A protein in kidney transplant patients. *Transplant Proc* 2000; **32**: 1796–1798.
31 Feussner G, Stech C, Dobmeyer J, Schaefer H, Otto G, Ziegler R. Serum amyloid A protein (SAA): a marker for liver allograft rejection in humans. *Clin Investig* 1994; **72**: 1007–1011.
32 Muller TF, Vogl M, Neumann MC, Lange H, Grimm M, Muller MM. Noninvasive monitoring using serum amyloid A and serum neopterin in cardiac transplantation. *Clin Chim Acta* 1998; **276**: 63–74.
33 Vermes E, Kirsch M, Farrokhi T, Loisance D, Fanen P, Zimmermann R. Serum amyloid A protein: not a relevant marker for recognition of cardiac allograft rejection. *Transplantation* 2004; **78**: 950–951.
34 Fuji S, Kim SW, Fukuda T, Mori S, Yamasaki S, Morita-Hoshi Y *et al.* Preengraftment serum C-reactive protein (CRP) value may predict acute graft-versus-host disease and nonrelapse mortality after allogeneic hematopoietic stem cell transplantation. *Biol Blood Marrow Transplant* 2008; **14**: 510–517.

blood

Prepublished online January 10, 2012;
doi:10.1182/blood-2011-07-368233

Impact of graft-versus-host disease on outcomes after allogeneic hematopoietic cell transplantation for adult T-cell leukemia: a retrospective cohort study

Junya Kanda, Masakatsu Hishizawa, Atae Utsunomiya, Shuichi Taniguchi, Tetsuya Eto, Yukiyoshi Moriuchi, Ryuji Tanosaki, Fumio Kawano, Yasushi Miyazaki, Masato Masuda, Koji Nagafuji, Masamichi Hara, Minoko Takanashi, Shunro Kai, Yoshiko Atsuta, Ritsuro Suzuki, Takakazu Kawase, Keitaro Matsuo, Tokiko Nagamura-Inoue, Shunichi Kato, Hisashi Sakamaki, Yasuo Morishima, Jun Okamura, Tatsuo Ichinohe and Takashi Uchiyama

Blood (print ISSN 0006-4971, online ISSN 1528-0020), is published weekly by the American Society of Hematology, 2021 L St, NW, Suite 900, Washington DC 20036.

Blood First Edition Paper, prepublished online January 10, 2012; DOI 10.1182/blood-2011-07-368233
From bloodjournal.hematologylibrary.org at SAGA DAIGAKU TOSHOKAN on January 10, 2012. For personal use only.

Impact of graft-versus-host disease on outcomes after allogeneic hematopoietic cell transplantation for adult T-cell leukemia: a retrospective cohort study

Junya Kanda,[1*] Masakatsu Hishizawa,[1*] Atae Utsunomiya,[2] Shuichi Taniguchi,[3] Tetsuya Eto,[4] Yukiyoshi Moriuchi,[5] Ryuji Tanosaki,[6] Fumio Kawano,[7] Yasushi Miyazaki,[8] Masato Masuda,[9] Koji Nagafuji,[10] Masamichi Hara,[11] Minoko Takanashi,[12] Shunro Kai,[13] Yoshiko Atsuta,[14] Ritsuro Suzuki,[14] Takakazu Kawase,[15] Keitaro Matsuo,[15] Tokiko Nagamura-Inoue,[16] Shunichi Kato,[17] Hisashi Sakamaki,[18] Yasuo Morishima,[19] Jun Okamura,[20] Tatsuo Ichinohe,[11] and Takashi Uchiyama[1**]

[1]Department of Hematology and Oncology, Graduate School of Medicine, Kyoto University, Kyoto, Japan; [2]Department of Hematology, Imamura Bun-in Hospital, Kagoshima, Japan; [3]Department of Hematology, Toranomon Hospital, Tokyo, Japan; [4]Department of Hematology, Hamanomachi Hospital, Fukuoka, Japan; [5]Department of Hematology, Sasebo City General Hospital, Sasebo, Japan; [6]Stem Cell Transplantation Unit, National Cancer Center Hospital, Tokyo, Japan; [7]Division of Internal Medicine, National Hospital Organization, Kumamoto Medical Center, Kumamoto, Japan; [8]Department of Hematology and Molecular Medicine Unit, Atomic Bomb Disease Institute, Nagasaki University Graduate School of Biomedical Science, Nagasaki, Japan; [9]Cancer Center, University Hospital, Faculty of Medicine, University of the Ryukyus, Nishihara, Japan; [10]Medicine and Biosystemic Science, Kyushu University Graduate School of Medical Sciences, Fukuoka, Japan; [11]Division of Hematology, Ehime Prefectural Central Hospital, Matsuyama, Japan; [12]Japasese Red Cross Tokyo Metropolitan Blood Center, Tokyo, Japan; [13]Department of Transfusion Medicine, Hyogo College of Medicine, Nishinomiya, Japan; [14]Department of Hematopoietic Stem Cell Transplantation Data Management, Nagoya University, School of Medicine, Nagoya, Japan; [15]Division of Epidemiology and Prevention, Aichi Cancer Center, Nagoya, Japan; [16]Department of Cell Processing and Transfusion, Research Hospital, Institute of Medical Science, University of Tokyo, Tokyo, Japan; [17]Department of Cell Transplantation and Regenerative Medicine, Tokai University, School of Medicine, Isehara, Japan; [18]Hematology Division, Tokyo Metropolitan Komagome Hospital, Tokyo, Japan; [19]Department of Hematology and Cell Therapy, Aichi Cancer Center Hospital, Nagoya, Japan; [20]Institute for Clinical Research, National Kyushu Cancer Center, Fukuoka, Japan.

*These two authors are contributed equally to this work.
**Deceased during the preparation of this manuscript.

Short running head: Impact of GVHD on allografting for ATL
Scientific category: Transplantation

†Corresponding author: Tatsuo Ichinohe, M.D.
Department of Hematology and Oncology, Graduate School of Medicine, Kyoto University, 54 Shogoin Kawaharacho, Sakyo-ku, Kyoto 606-8507, Japan.
Tel: +81-75-751-3153; Fax: +81-75-751-4963; e-mail: nohe@kuhp.kyoto-u.ac.jp

Abstract

Allogeneic hematopoietic cell transplantation (HCT) is an effective treatment for adult T-cell leukemia (ATL), raising the question about the role of graft-versus-leukemia effect against ATL. In this study, we retrospectively analyzed the effects of acute and chronic graft-versus-host disease (GVHD) on overall survival, disease-associated mortality, and treatment-related mortality among 294 ATL patients who received allogeneic HCT and survived at least 30 days post-transplant with sustained engraftment. Multivariable analyses treating the occurrence of GVHD as a time-varying covariate demonstrated that the development of grade 1-2 acute GVHD was significantly associated with higher overall survival [hazard ratio (HR) for death, 0.65, p=0.018] compared with the absence of acute GVHD. Occurrence of either grade 1-2 or grade 3-4 acute GVHD was associated with lower disease-associated mortality compared with the absence of acute GVHD, while grade 3-4 acute GVHD was associated with a higher risk for treatment-related mortality (HR 3.50, p<0.001). The development of extensive chronic GVHD was associated with higher treatment-related mortality (HR 2.75, p=0.006) compared with the absence of chronic GVHD. Collectively, these results indicate that the development of mild-to-moderate acute GVHD confers a lower risk of disease progression and a beneficial influence on survival of allografted patients with ATL.

From bloodjournal.hematologylibrary.org at SAGA DAIGAKU TOSHOKAN on January 10, 2012. For personal use only.

Introduction

Adult T-cell leukemia (ATL) is a mature T-cell neoplasm that is causally associated with a retrovirus designated human T-cell leukemia virus type I (HTLV-I).[1-4] HTLV-I is endemic in southwestern Japan, sub-Saharan Africa, the Caribbean Basin, and South America.[3,4] In Japan, more than one million people were estimated to be infected with HTLV-I. Although the majority of HTLV-I-infected individuals remain asymptomatic throughout their lives, about 5% develop ATL at a median age of 40 to 60 years.[4,5]

ATL is categorized into four clinical variants according to its clinical features: smoldering, chronic, acute, and lymphoma types.[6] The acute and lymphoma variants of ATL have an extremely poor prognosis mainly because of resistance to a variety of cytotoxic agents and susceptibility to opportunistic infections; the median survival time is approximately 13 months with conventional chemotherapy,[7,8] although encouraging results have been recently reported with the use of novel agents such as mogamulizumab.[9-11]

Over the past decade, allogeneic hematopoietic cell transplantation (HCT) has been increasingly performed with the aim of improving dismal prognosis of patients who developed ATL.[12-18] Notably, some patients with ATL who relapsed after allogeneic HCT were shown to achieve remission only with the cessation of immunosuppressive agents, raising the question of whether the graft-versus-leukemia effect against ATL can be induced as part of graft-versus-host reaction.[19,20] In one study, among 10 patients who experienced relapse of ATL after transplantation and were withdrawn from immunosuppressive therapy, 8 developed graft-versus-host disease (GVHD)

and 6 of them subsequently achieved complete remission of ATL.[19] Similar observations have been rarely reported in other aggressive mature lymphoid neoplasms,[21] suggesting the unique susceptibility of ATL to graft-versus-host reactions. Recently, a combined analysis of two prospective studies including a total of 29 ATL patients undergoing allogeneic HCT suggested that development of mild acute GVHD favorably affected overall survival and progression-free survival.[22] However, the impact of GVHD on the outcome of allogeneic HCT in ATL needs to be verified in a much larger cohort. We previously conducted a nationwide retrospective study to evaluate the current results of allogeneic HCT for ATL, and confirmed that a substantial proportion of patients with ATL can enjoy long-term disease-free survival after transplantation; the overall survival rates at 3 years among patients who received transplants in complete remission and not in complete remission were 51% and 26%, respectively.[23] Using the same cohort, we further evaluated the effects of acute and chronic GVHD on long-term outcomes of allografted patients with ATL.

Methods

Collection of data

Data on 417 patients with acute or lymphoma type ATL who had undergone allogeneic bone marrow, peripheral blood, or cord blood transplantation between January 1, 1996, and December 31, 2005, were collected through the Japan Society for Hematopoietic Cell Transplantation (JSHCT), the Japan Marrow Donor Program (JMDP), and the Japan Cord Blood Bank Network (JCBBN), the

From bloodjournal.hematologylibrary.org at SAGA DAIGAKU TOSHOKAN on January 10, 2012. For personal use only.

three largest HCT registries in our country; their roles were detailed elsewhere.[23] The patients were included from 102 transplant centers; the data were updated as of December 2008. The study was approved by the data management committees of JSHCT, JMDP, and JCBBN, as well as by the institutional review boards of Kyoto University, Graduate School of Medicine, where this study was organized.

Inclusion and exclusion criteria

Patients were included in the analysis if the following data were available: age at transplantation, sex of the recipient, donor type, stem cell source, agents used in the conditioning regimen and GVHD prophylaxis, the maximum grade and day of occurrence of acute GVHD, and the day of neutrophil recovery. Acute GVHD was reported according to the traditional criteria,[24] except that one patient was considered to have late-onset acute GVHD at day 133; neutrophil recovery was considered to have occurred when an absolute neutrophil count exceeded 0.5 $x10^9$/L for three consecutive days following transplantation. Patients who missed any of these data (n=37), who had a history of prior autologous or allogeneic HCT (n=8), who had received an ex vivo T-cell-depleted graft (n=1), who experienced primary or secondary graft failure (n=24) were excluded from the analysis. Since the association between the occurrence of acute GVHD and disease-associated mortality was difficult to evaluate in the event of early toxic death, patients who died within 30 days of transplantation (n=53) were also excluded from the study. Among these 53 patients, 22 were evaluable for acute GVHD: grade 0 in 17, grade 1-2 in 3, and grade 3-4 in 2 patients. Two physicians

(J.K. and T.I.) independently reviewed the quality of collected data, and a total of 294 patients (158 males and 136 females), with a median age of 51 years (range, 18-79), were found to meet these criteria and included in the study: 163 patients from JSHCT, 82 from JMDP, and 49 from JCBBN. No overlapping cases were identified. Of these 294 patients, the effects of chronic GVHD, which was reported and graded according to traditional criteria,[25] were considered evaluable for the 183 patients who survived at least 100 days after transplantation with complete information on the type and the day of occurrence of chronic GVHD.

Endpoints

The primary endpoint of the study was the effect of acute GVHD on overall survival, which was defined as the period from the date of transplantation until the date of death from any cause or the last follow-up. The secondary endpoints of the study included the impact of acute GVHD on disease-associated and treatment-related mortality, and the impact of chronic GVHD on overall survival, disease-associated mortality, and treatment-related mortality. Reported causes of death were reviewed and categorized into disease-associated or treatment-associated deaths. Disease-associated deaths were defined as deaths from relapse or progression of ATL, while treatment-related deaths were defined as any death other than disease-associated deaths.

Statistical analysis

The probability of overall survival was estimated by the Kaplan-Meier method.

From bloodjournal.hematologylibrary.org at SAGA DAIGAKU TOSHOKAN on January 10, 2012. For personal use only.

Treatment-related and disease-associated mortality were estimated with the use of cumulative incidence curves to accommodate the following competing events[26]: disease-associated death for treatment-related mortality and treatment-related deaths for disease-associated mortality. Data on patients who were alive at the time of last follow-up were censored. Semi-landmark plots were used to illustrate the effects of GVHD on overall survival and cumulative incidence of disease-associated and treatment-related deaths. For patients with acute or chronic GVHD, the probability of overall survival and the cumulative incidences of disease-associated and treatment-related deaths were plotted as a function of time from the onset of acute or chronic GVHD. Day 24.5, which was the median day of onset for acute GVHD, was termed as the landmark day in patients without acute GVHD. In the case of patients without chronic GVHD, day 116, which was the median day of onset for chronic GVHD, was termed as the landmark day.

Univariable and multivariable Cox proportional–hazards regression models were used to evaluate variables potentially affecting overall survival, while the Fine and Gray proportional subdistribution hazards models were used to evaluate variables potentially affecting disease-associated and treatment-related mortality.[27] In these regression models, the occurrence of acute and chronic GVHD was treated as a time-varying covariate.[28] In the analysis of acute GVHD, patients were assigned to the "no acute GVHD group" at the time of transplantation and then transferred to the "grade 1 or 2 acute GVHD group" or to the "grade 3 or 4 acute GVHD group" at the onset of the maximum grade of acute GVHD. In the analysis of chronic GVHD, patients were assigned to the "no